

**NASA TECHNICAL  
MEMORANDUM**



**N73-14005**  
**NASA TM X-2701**

**NASA TM X-2701**

**CASE FILE  
COPY**

**LOW SUBSONIC AERODYNAMIC  
CHARACTERISTICS OF A SHUTTLE ORBITER  
HAVING 35° TRAPEZOIDAL WING  
AND 75° INBOARD GLOVE**

*by Bernard Spencer, Jr., and George M. Ware*

*Langley Research Center*

*Hampton, Va. 23365*

1. Report No. NASA TM X-2701	2. Government Accession No.	3. Recipient's Catalog No.	
4. Title and Subtitle LOW SUBSONIC AERODYNAMIC CHARACTERISTICS OF A SHUTTLE ORBITER HAVING 35° TRAPEZOIDAL WING AND 75° INBOARD GLOVE		5. Report Date January 1973	
		6. Performing Organization Code	
7. Author(s) Bernard Spencer, Jr., and George M. Ware		8. Performing Organization Report No. L-8674	
		10. Work Unit No. 502-37-01-01	
9. Performing Organization Name and Address NASA Langley Research Center Hampton, Va. 23365		11. Contract or Grant No.	
		13. Type of Report and Period Covered Technical Memorandum	
12. Sponsoring Agency Name and Address National Aeronautics and Space Administration Washington, D.C. 20546		14. Sponsoring Agency Code	
15. Supplementary Notes			
16. Abstract  <p>An investigation has been made in the Langley low-turbulence pressure tunnel to determine the subsonic aerodynamic characteristics of a 0.01875-scale model of a shuttle orbiter configuration having a 35° swept trapezoidal wing and 75° swept fixed glove located ahead of the wing. Tests were made at Mach numbers below 0.30 and Reynolds numbers, based on body length, from <math>12.32 \times 10^6</math> to <math>24.65 \times 10^6</math>, with most of the tests being made at a Reynolds number of <math>12.32 \times 10^6</math>. Variables investigated included configuration components in combination, elevon deflections and rudder deflections in combination, and dorsal-tail roll-out angle.</p>			
17. Key Words (Suggested by Author(s))  Space shuttle Wing gloves Orbiter aerodynamics		18. Distribution Statement  Unclassified - Unlimited	
19. Security Classif. (of this report) Unclassified	20. Security Classif. (of this page) Unclassified	21. No. of Pages 42	22. Price* \$3.00

LOW SUBSONIC AERODYNAMIC CHARACTERISTICS  
OF A SHUTTLE ORBITER HAVING 35° TRAPEZOIDAL WING  
AND 75° INBOARD GLOVE

By Bernard Spencer, Jr., and George M. Ware  
Langley Research Center

SUMMARY

An investigation has been made in the Langley low-turbulence pressure tunnel to determine the subsonic aerodynamic characteristics of a 0.01875-scale model of a shuttle orbiter configuration having a 35° swept trapezoidal wing and 75° swept fixed glove located ahead of the wing. Tests were made at Mach numbers below 0.30 and Reynolds numbers, based on body length, from  $12.32 \times 10^6$  to  $24.65 \times 10^6$ , with most of the tests being made at a Reynolds number of  $12.32 \times 10^6$ . Variables investigated included configuration components in combination, elevon deflections and rudder deflections in combination, and twin-dorsal-tail roll-out angle.

The results of the investigation indicate large favorable lift produced by the wing glove at desired angles for landing (i.e., 17°), but pitch-up occurred because of excessive glove area. The baseline configuration, which had twin dorsal tails rolled out 30° from the vertical, was longitudinally stable (static margin of 1.2 percent) about the design center-of-gravity location of 0.70 body length. Maximum trimmed lift-drag ratio for the baseline configuration was about 6.7 at a lift coefficient of 0.38. Decreasing the tail roll-out angle to 15° resulted in a configuration that was neutrally stable longitudinally, and using a center vertical tail resulted in a configuration that was unstable longitudinally. The baseline configuration with dorsal tails at 30° roll-out was approximately neutrally stable directionally. Setting the tail roll-out to 15° provided some directional stability for the test angle-of-attack range. The use of a single center-line tail of approximately the same area as the total area of the twin tails provided considerable increase in directional stability without greatly increasing positive effective dihedral.

INTRODUCTION

The National Aeronautics and Space Administration is continuing analytical and experimental studies related to the development of design criteria for space shuttle orbiter configurations suitable for transportation of large payloads to and from near-earth orbit. One such concept designed at the NASA Manned Spacecraft Center has a

35° trapezoidal wing with a 75° fixed glove forming a cranked planform wing and body-mounted twin dorsal tails. The primary reason for incorporating a wing glove was to control the location of the aerodynamic center during vehicle design iterations by varying the glove size. An interesting characteristic of wing designs of this type is the large incremental lift provided by the glove at moderate to high angles of attack over that obtained on a basic trapezoidal wing. (See ref. 1.) This effect is quite favorable in producing the lift necessary to reduce landing speeds. However, excessive glove size may result in pitch-up, depending on basic wing pitch characteristics. (See refs. 2 and 3.)

The purpose of the present study is to examine the low subsonic stability and control characteristics of a 0.01875-scale model of the concept as presently configured, as well as the lift benefits of the wing glove. The configuration of this investigation is considered in the return-from-orbit glide mode (i.e., unpowered flight). Both static longitudinal and summary lateral-directional characteristics have been determined in the Langley low-turbulence pressure tunnel at Reynolds numbers, based on body length, from  $12.32 \times 10^6$  to  $24.65 \times 10^6$  at Mach numbers below 0.30. Angle of attack was varied from about -3° to 22° at angles of sideslip of 0° and 5°.

## SYMBOLS

The longitudinal characteristics are presented about the stability axes, and the lateral-directional characteristics are presented about the body axes. All coefficients are normalized with respect to the projected planform area, mean aerodynamic chord, and span of the trapezoidal wing alone. (See table I.) The moment reference point corresponds to a longitudinal center-of-gravity location at 0.70 body length and a vertical location on the body center line. (See fig. 1.)

Values are given in both SI and U.S. Customary Units. The measurements and calculations were made in U.S. Customary Units.

b span of trapezoidal wing

$C_D$  drag coefficient,  $\frac{\text{Drag}}{q_\infty S}$

$C_L$  lift coefficient,  $\frac{\text{Lift}}{q_\infty S}$

$C_l$  rolling-moment coefficient,  $\frac{\text{Rolling moment}}{q_\infty S b}$

$C_{l_\beta} = \frac{\Delta C_l}{\Delta \beta}$ , per deg



$C_m$	pitching-moment coefficient, $\frac{\text{Pitching moment}}{q_\infty S \bar{c}}$
$C_n$	yawing-moment coefficient, $\frac{\text{Yawing moment}}{q_\infty S b}$
$C_{n\beta} = \frac{\Delta C_n}{\Delta \beta}$ , per deg	
$C_Y$	side-force coefficient, $\frac{\text{Side force}}{q_\infty S}$
$C_{Y\beta} = \frac{\Delta C_Y}{\Delta \beta}$ , per deg	
$\bar{c}$	mean aerodynamic chord of trapezoidal wing
$L/D$	lift-drag ratio
$l$	actual body length
$q_\infty$	dynamic pressure
$R$	Reynolds number based on body length
$S$	total projected planform area of trapezoidal wing alone
$\alpha$	angle of attack, deg
$\beta$	angle of sideslip, deg
$\delta_e$	elevon deflection angle (positive when trailing edge deflected down), deg
$\delta_f$	base-flap deflection angle (positive when trailing edge deflected down), deg
$\delta_r$	rudder deflection angle measured normal to hinge line (positive with trailing edge left), deg
$\phi$	dorsal-tail roll-out angle, deg

Subscripts:

L            left

R            right

## DESCRIPTION OF MODEL

Sketches and photographs of the 0.01875-scale model used in the present investigation are presented in figures 1 and 2, respectively. The baseline configuration consisted of a body, a  $35^\circ$  swept trapezoidal wing with a fixed  $75^\circ$  swept inboard glove, and twin body-mounted dorsal tails rolled out  $30^\circ$  from the vertical. A more detailed description of the model components is listed in table I. Variations from the baseline configuration consisted of the twin dorsal tails set at a roll-out angle of  $15^\circ$  and the use of a single center-line vertical tail having 93 percent of the total area of the dorsal tails. Rudders located on the twin tails could be deflected as a pair at  $5^\circ$  each for yaw control or differentially ( $\delta_{r,L} = -5^\circ$  and  $\delta_{r,R} = 5^\circ$ ) for additional pitch control. Elevons located on the trapezoidal wing could be set at deflections of  $0^\circ$ ,  $-2.5^\circ$ ,  $-5.0^\circ$ , and  $-10^\circ$ . An additional control surface in the form of a base flap was investigated at  $0^\circ$  and  $-10^\circ$  deflection. However, the base flap was not considered as part of the baseline configuration. Wing-mounted tip pods (attitude control propulsion systems (ACPS)) were considered as part of the baseline configuration. (See fig. 1.)

## TESTS AND CORRECTIONS

Tests were made in the Langley low-turbulence pressure tunnel at Mach numbers below 0.30 and Reynolds numbers, based on body length, from  $12.32 \times 10^6$  to  $24.65 \times 10^6$ , with most being conducted at  $12.32 \times 10^6$ . The angle of attack was generally varied from about  $-3^\circ$  to  $22^\circ$  at  $0^\circ$  and  $5^\circ$  of sideslip.

The model was sting supported, and forces and moments were measured by use of a six-component strain-gage balance. Angle of attack has been corrected for the effects of sting and balance deflection under load. Lift interference and tunnel blockage effects have been applied to the data by use of the methods described in references 4 and 5, respectively. The data presented herein represent gross drag in that base drag is included.

## RESULTS AND DISCUSSION

Basic longitudinal aerodynamic characteristics are presented in figures 3 to 9, and summary lateral-directional stability characteristics are presented in figures 10 and 11.

Increasing Reynolds number from  $12.32 \times 10^6$  to  $24.65 \times 10^6$  on the baseline configuration (fig. 3) shows little or no effect on the longitudinal aerodynamic characteristics. Therefore, to expedite testing, the lowest Reynolds number was selected for the rest of the investigation.

Longitudinal control effectiveness (fig. 4) is excessive, as would be expected, because of the extremely large elevons of the configuration. An elevon deflection of  $-2.5^\circ$  was sufficient to trim the model to an angle of attack of  $16.5^\circ$ . However, the vehicle indicates pitch-up at this trim angle of attack, with increasing instability accompanying further increases in  $\alpha$ . This suggests excessive glove area. Calculation of configuration aspect ratio and effective quarter-chord sweep of the trapezoidal wing-glove combination shows this vehicle to fall in the region of decreasing longitudinal stability with increasing lift shown in the pitch-up boundary charts of reference 3.

Employing baseline twin-dorsal-tail rudders to provide additional trim (fig. 5) shows little or no pitch control effectiveness for the  $5^\circ$  deflection. A comparison of base-flap control effectiveness with that of the wing elevons is presented in figure 6. Adding the undeflected base flap produced no change on the longitudinal characteristics of the vehicle; however, it is interesting to note that  $\delta_f = -10^\circ$  provides trim to  $\alpha \approx 12^\circ$  and  $\Delta C_m$  values approximately half those obtained with  $-2.5^\circ$  deflection of the large elevons, with no change in the value of maximum  $L/D$ .

Longitudinal aerodynamic characteristics associated with various vertical-tail arrangements on the wing-body configuration having  $\delta_e = -2.5^\circ$  (fig. 7) show losses in maximum  $L/D$  of about 0.40 due to the addition of the  $\phi = 30^\circ$  twin dorsal tails or the single vertical tail. However, changing twin-dorsal-tail roll-out to  $15^\circ$  results in an 0.80 loss in maximum  $L/D$  due to higher  $C_D$  resulting from mutual flow-field interference as the tails come closer together and the reduced lift component as  $\phi$  is reduced to  $15^\circ$ . The addition of twin dorsal tails increased the static margin of the wing-body combination about 2 percent. Therefore, the baseline configuration had a 1.2 percent static margin about the design center-of-gravity position of 0.70 body length. Reducing the roll-out angle to  $15^\circ$  reduced the static margin to near zero, and with the center vertical tail or with tails off, the configuration was longitudinally unstable in the moderate lift range.

The effects of the wing ACPS pods on the longitudinal aerodynamic characteristics of the baseline configuration having  $\delta_e = -2.5^\circ$  are presented in figure 8. These data indicate that removing the pods resulted in a more linear  $C_L$  and  $C_m$  variation with angle of attack prior to the onset of pitch-up and a reduction in drag over the test angle-of-attack range. The model with pods off had a value of maximum lift-drag ratio of about 7.1 compared with 6.7 with pods on.

Figure 9 shows the effects of removing the  $75^\circ$  swept glove from the trapezoidal wing. The large favorable lift of the glove particularly at the higher angles of attack is evident, as has been noted in reference 1. An examination of the trapezoidal-wing-alone characteristics shows the typical breakover in  $C_L$  at  $\alpha$  above approximately  $12^\circ$  and the resultant pitch-down characteristics for this type of wing. Although the lift of the glove is favorable, the destabilizing effect is large, especially at the higher angles of attack, and therefore reduction in glove size appears to be a means of alleviating configuration pitch-up and increasing longitudinal stability. Removing the wing glove also resulted in an increase in maximum untrimmed  $L/D$  from 6.7 to 7.2. The higher lift-drag ratios are primarily due to more efficient drag due to lift associated with the higher aspect ratio of the trapezoidal wing alone.

Figures 10 and 11 present the effects of the addition of the vertical tail and twin dorsal tails on the lateral-directional stability characteristics of the complete wing-body vehicle with wing glove on and off, respectively. These data were obtained by taking the difference in lateral coefficients measured at angles of sideslip of  $0^\circ$  and  $5^\circ$  over the test angle-of-attack range and therefore do not account for any nonlinearities which may occur in the intermediate  $\beta$  range. While the baseline glove-on configuration with the  $\phi = 30^\circ$  twin dorsal tails indicated approximately neutral directional stability, decreasing tail roll-out to  $\phi = 15^\circ$  is noted to provide moderate positive values of  $C_{n\beta}$  except near  $\alpha = 12^\circ$  throughout the test angle-of-attack range. The use of a single center-line vertical tail of comparable size provided a considerable increase in directional stability without greatly increasing positive effective dihedral.

The trend of the data for the model with wing glove removed in figure 11 follows that of the configurations with the glove on. There was a slight overall increase in directional stability caused by the removal of wing area ahead of the center of gravity. The most significant difference between the glove-on and glove-off data is the large positive shift in  $C_{l\beta}$  (loss in positive effective dihedral) when the glove was removed. This effect is caused by the reduction in effective wing sweep and has been previously shown in reference 6.

## SUMMARY OF RESULTS

Subsonic wind-tunnel tests have been made to determine the static longitudinal and lateral aerodynamic characteristics of a shuttle orbiter configuration having a  $35^\circ$  swept trapezoidal wing and a  $75^\circ$  swept fixed glove located ahead of the wing and twin dorsal tails rolled out  $30^\circ$ . The results of the investigation may be summarized as follows:

1. The wing glove produced large favorable lift at the desired angles of attack for landing (i.e.,  $17^\circ$ ), but pitch-up occurred because of the excessive glove area. The maxi-

mum trimmed lift-drag ratio for the baseline configuration was about 6.7 at a lift coefficient of 0.38.

2. The baseline configuration which had twin tails rolled out  $30^\circ$  was longitudinally stable about the design center-of-gravity location of 0.70 body length. Decreasing the tail roll-out angle to  $15^\circ$  resulted in a configuration that was neutrally stable longitudinally, and using a center vertical tail resulted in a configuration that was unstable longitudinally.

3. The baseline configuration had about neutral directional stability. Decreasing twin-dorsal-tail roll-out angle to  $15^\circ$  provided some directional stability, and the use of a center tail with approximately the same area as the twin tails provided a considerable increase in stability without greatly increasing positive effective dihedral.

Langley Research Center,  
National Aeronautics and Space Administration,  
Hampton, Va., December 6, 1972.

#### REFERENCES

1. Ray, Edward J.; McKinney, Linwood W.; and Carmichael, Julian G.: Maneuver and Buffet Characteristics of Fighter Aircraft. Presented at AGARD Specialists' Meeting on Fluid Dynamics of Aircraft Stalling (Lisbon, Portugal), Apr. 26-28, 1972.
2. Hopkins, Edward J.; Hicks, Raymond M.; and Carmichael, Ralph L.: Effects of Planform Variations on the Aerodynamic Characteristics of Low-Aspect-Ratio Wings With Cranked Leading Edges. Conference on Aircraft Aerodynamics, NASA SP-124, 1966, pp. 469-483.
3. Spreemann, Kenneth P.: Design Guide for Pitch-Up Evaluation and Investigation at High Subsonic Speeds of Possible Limitations Due to Wing-Aspect-Ratio Variations. NASA TM X-26, 1959.
4. Swanson, Robert S.; and Toll, Thomas A.: Jet-Boundary Corrections for Reflection-Plane Models in Rectangular Wind Tunnels. NACA Rep. 770, 1943. (Supersedes NACA WR L-458.)
5. Herriot, John G.: Blockage Corrections for Three-Dimensional-Flow Closed-Throat Wind Tunnels, With Consideration of the Effect of Compressibility. NACA Rep. 995, 1950. (Supersedes NACA RM A7B28.)
6. Tosti, Louis P.: Low-Speed Static Stability and Damping-in-Roll Characteristics of Some Swept and Unswept Low-Aspect-Ratio Wings. NACA TN 1468, 1947.

TABLE I. - GEOMETRIC CHARACTERISTICS OF 0.01875-SCALE MODEL

## Body:

Overall length, cm (in.) . . . . .	62.611 (24.650)
Maximum height, cm (in.) . . . . .	10.769 (4.240)
Maximum width, cm (in.) . . . . .	9.955 (3.919)

## Wing (35° trapezoid only):

Root chord, cm (in.) . . . . .	35.719 (14.063)
Tip chord, cm (in.) . . . . .	7.138 (2.810)
Mean aerodynamic chord, cm (in.) . . . . .	24.148 (9.507)
Span, <sup>a</sup> cm (in.) . . . . .	53.109 (20.909)
Total planform area, <sup>a</sup> m <sup>2</sup> (ft <sup>2</sup> ) . . . . .	0.111 (1.202)
Elevon total planform area, m <sup>2</sup> (ft <sup>2</sup> ) . . . . .	0.027 (0.293)
Leading-edge sweep, deg . . . . .	35
Trailing-edge sweep, deg . . . . .	-19.6
Dihedral, deg . . . . .	7
Incidence, deg . . . . .	1.5
Airfoil section . . . . .	NACA 0008-64
Aspect ratio . . . . .	2.525
Taper ratio . . . . .	0.20

## Wing-glove combination (35° trapezoid with 75° glove):

Root chord, cm (in.) . . . . .	71.152 (28.013)
Mean aerodynamic chord, cm (in.) . . . . .	40.862 (16.088)
Total planform area, m <sup>2</sup> (ft <sup>2</sup> ) . . . . .	0.150 (1.619)
Leading-edge sweep, deg . . . . .	75/35
Dihedral, deg . . . . .	7
Incidence, deg . . . . .	1.5
Airfoil section . . . . .	NACA 0005 (inboard)
Aspect ratio . . . . .	1.875
Taper ratio . . . . .	0.100

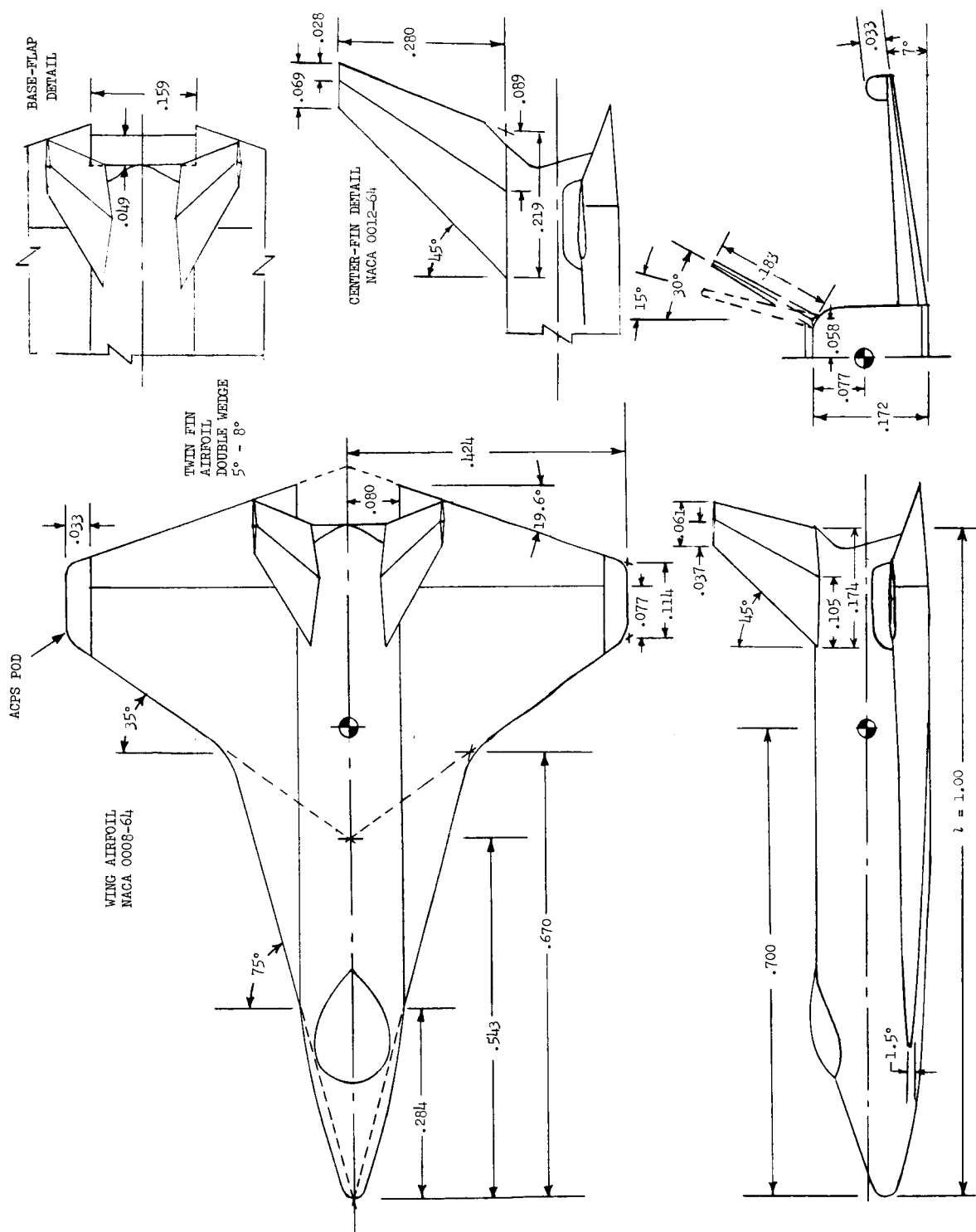
## Twin dorsal tails (each):

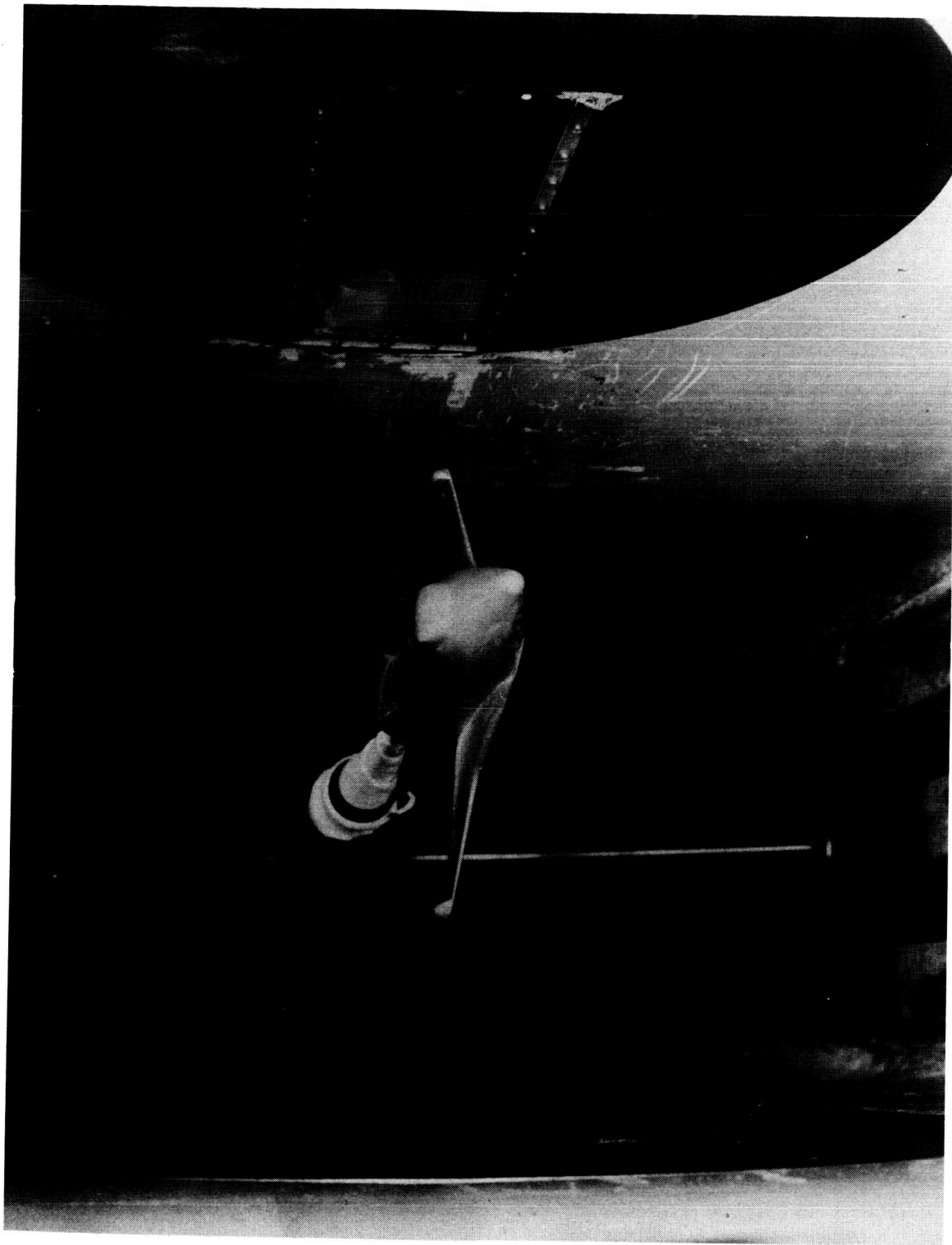
Root chord (exposed), cm (in.) . . . . .	10.955 (4.313)
Tip chord, cm (in.) . . . . .	3.810 (1.500)
Span (exposed), cm (in.) . . . . .	11.430 (4.500)
Area (exposed), m <sup>2</sup> (ft <sup>2</sup> ) . . . . .	0.0083 (0.089)
Area, rudder (exposed), m <sup>2</sup> (ft <sup>2</sup> ) . . . . .	0.0032 (0.0348)
Rudder hinge line . . . . .	60% chord
Leading-edge sweep, deg . . . . .	45
Trailing-edge sweep, deg . . . . .	20.55
Airfoil section . . . . .	Wedge 5° to 60% chord Wedge -8° from 60% to 100% chord
Aspect ratio . . . . .	1.575
Taper ratio . . . . .	0.348

## Center vertical tail:

Root chord (exposed), cm (in.) . . . . .	13.712 (5.398)
Tip chord, cm (in.) . . . . .	4.320 (1.700)
Span (exposed), cm (in.) . . . . .	17.531 (6.902)
Area (exposed), m <sup>2</sup> (ft <sup>2</sup> ) . . . . .	0.016 (0.1701)
Area, rudder (exposed), m <sup>2</sup> (ft <sup>2</sup> ) . . . . .	0.0064 (0.069)
Leading-edge sweep, deg . . . . .	45
Trailing-edge sweep, deg . . . . .	25
Airfoil section . . . . .	NACA 0012-64
Aspect ratio . . . . .	1.945
Taper ratio . . . . .	0.315

<sup>a</sup> Model reference dimensions.





L-72-4206

(a) Three-quarter front view from above.

Figure 2.- Photographs of model mounted in low-turbulence pressure tunnel.

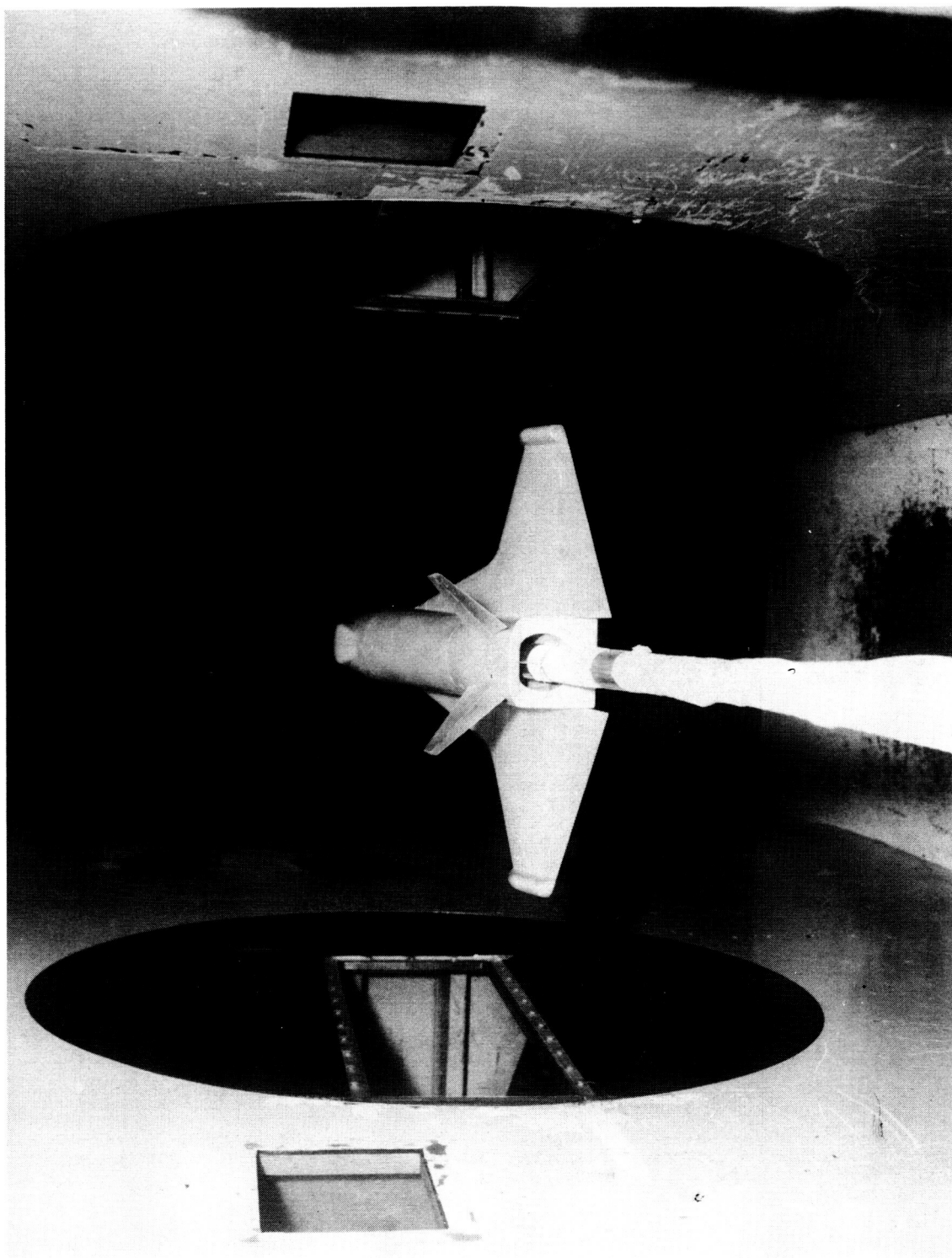




L-72-4207

(b) Three-quarter front view from below.

Figure 2.- Continued.



L-72-4208

(c) Rear view from above.

Figure 2. - Concluded.

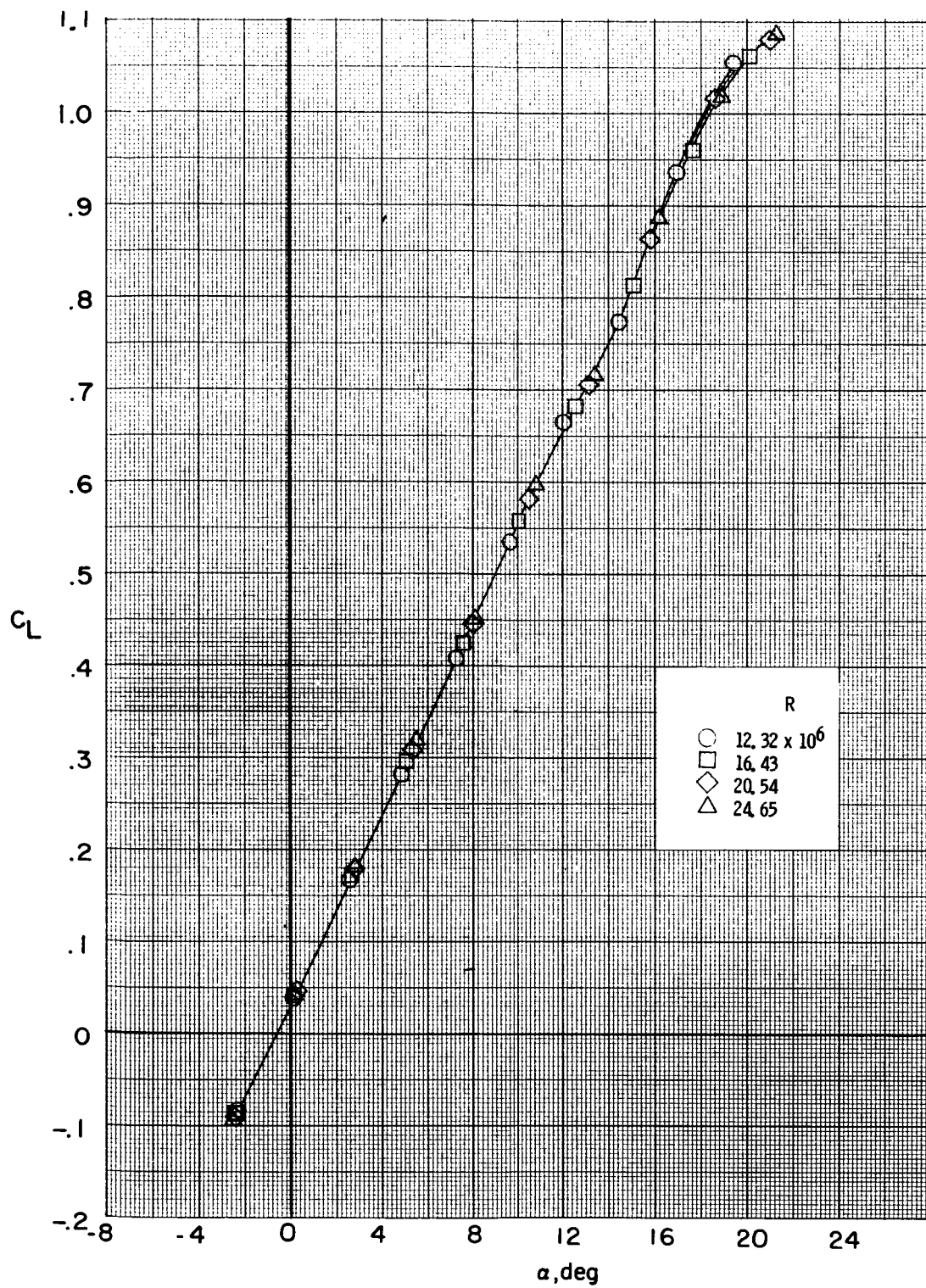


Figure 3.- Effects of Reynolds number on longitudinal aerodynamic characteristics of baseline model.  $\beta = 0^\circ$ ;  $\delta_e = 0^\circ$ .

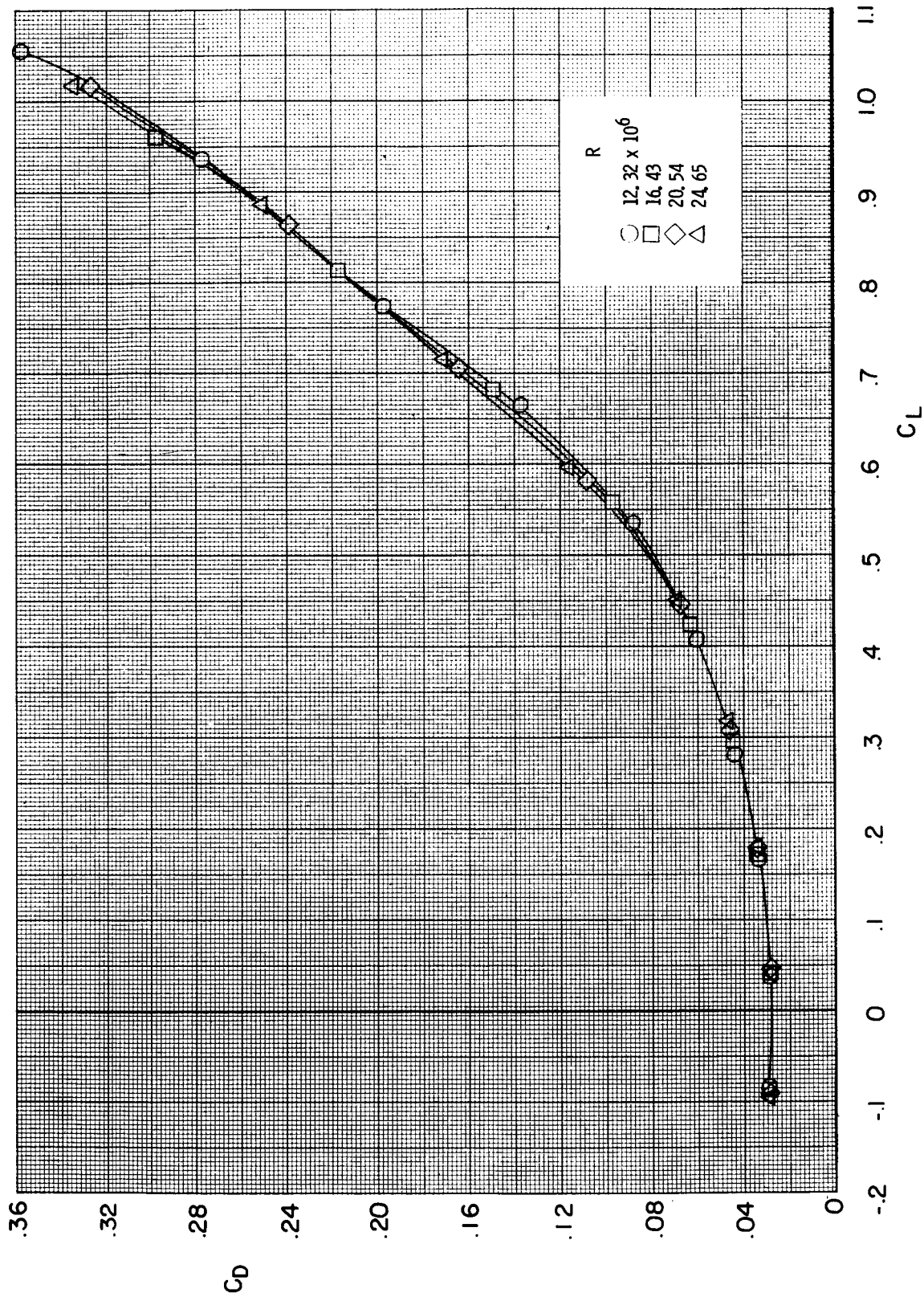


Figure 3.- Continued.

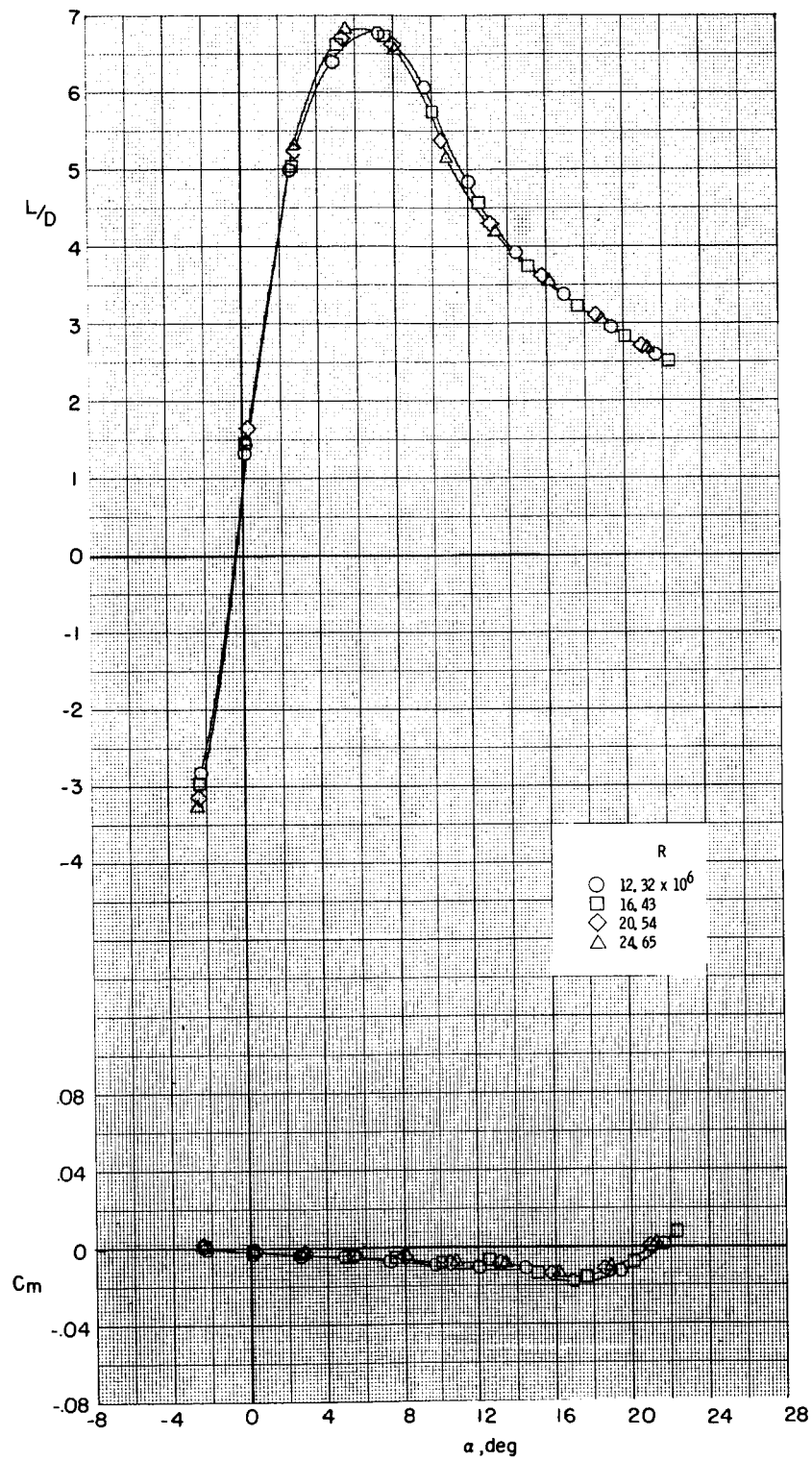


Figure 3.- Continued.

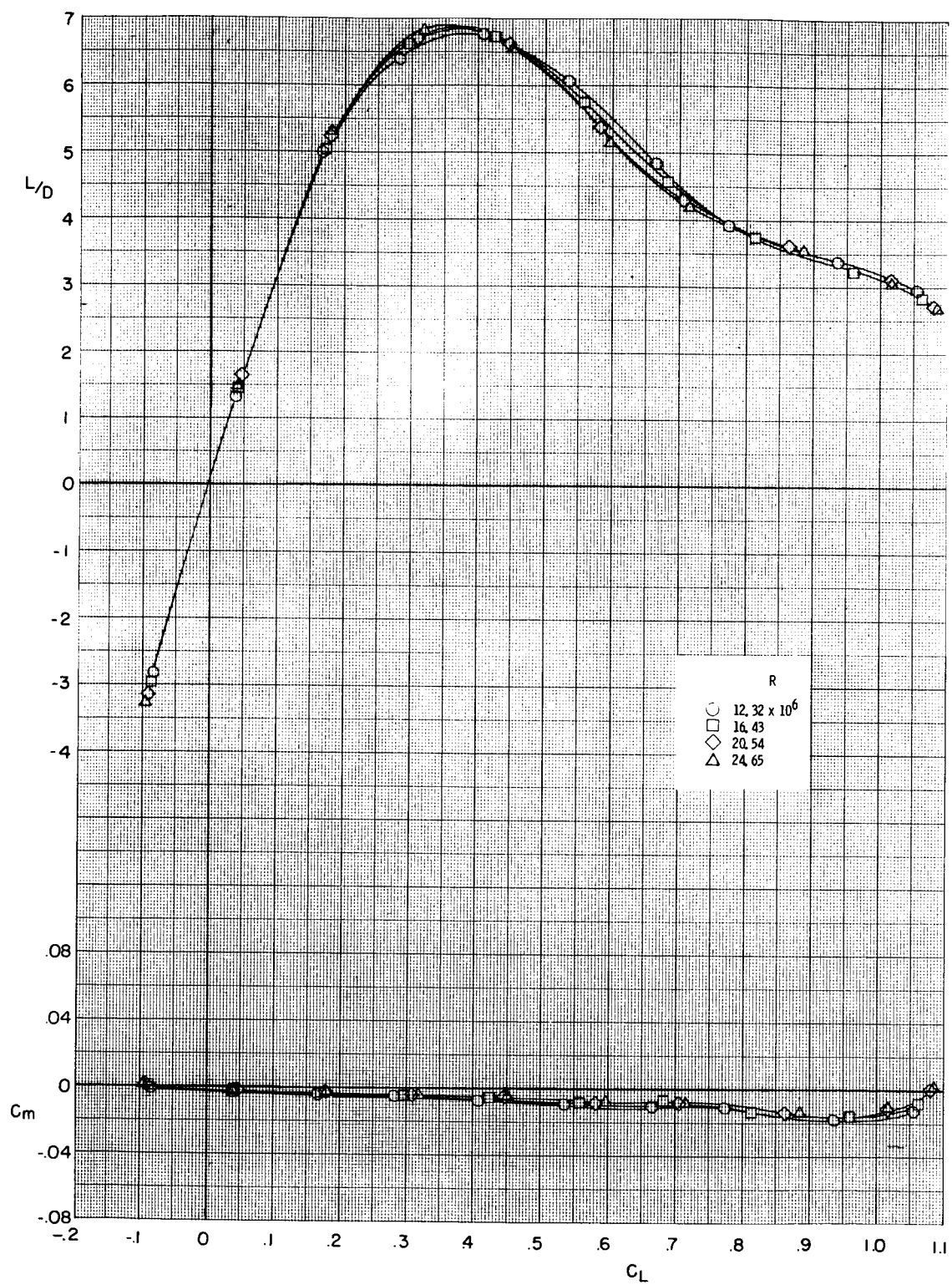


Figure 3.- Concluded.



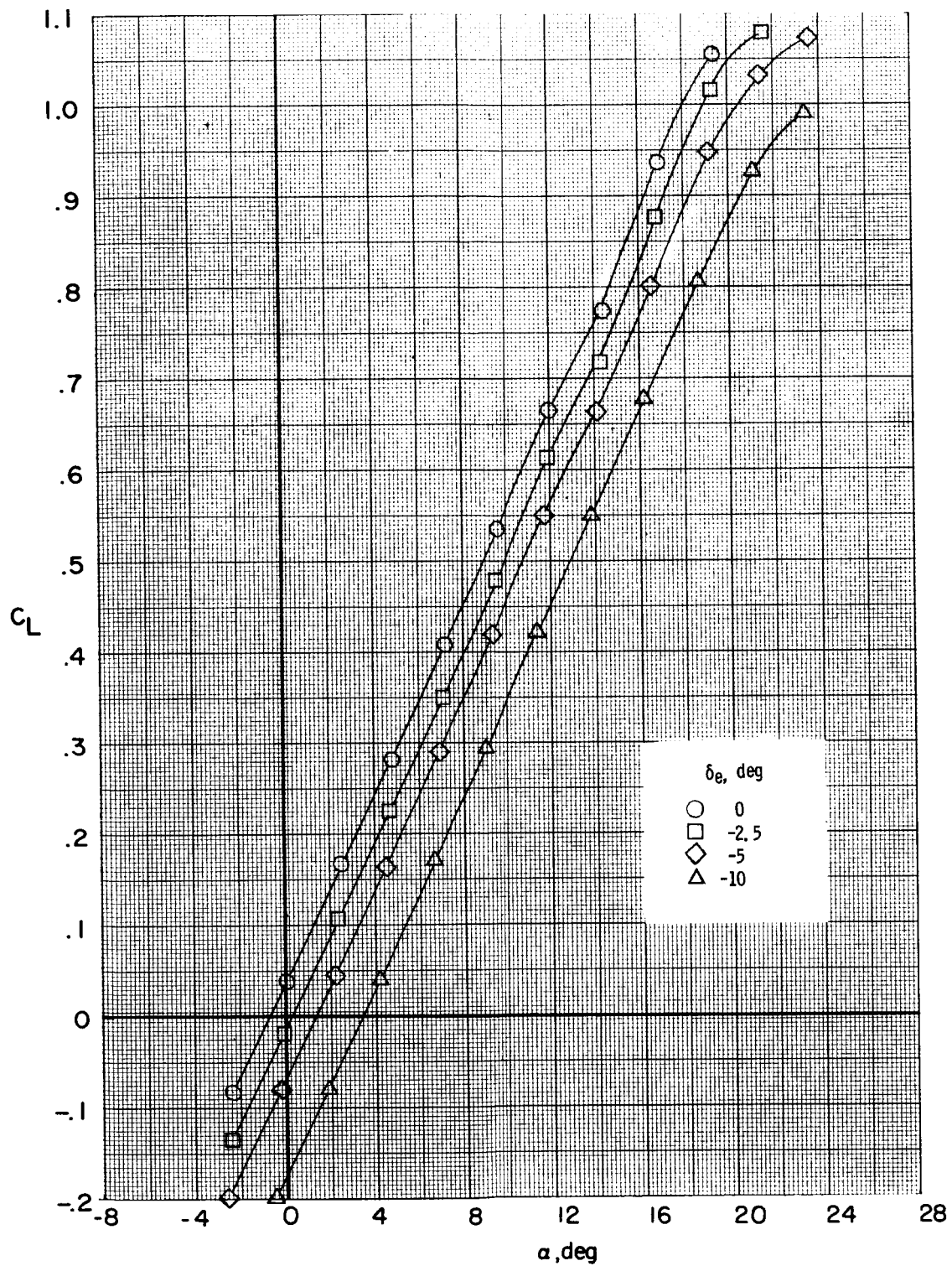


Figure 4.- Effects of elevon deflection on longitudinal aerodynamic characteristics of baseline model.  $R = 12.32 \times 10^6$ ;  $\beta = 0^\circ$ .

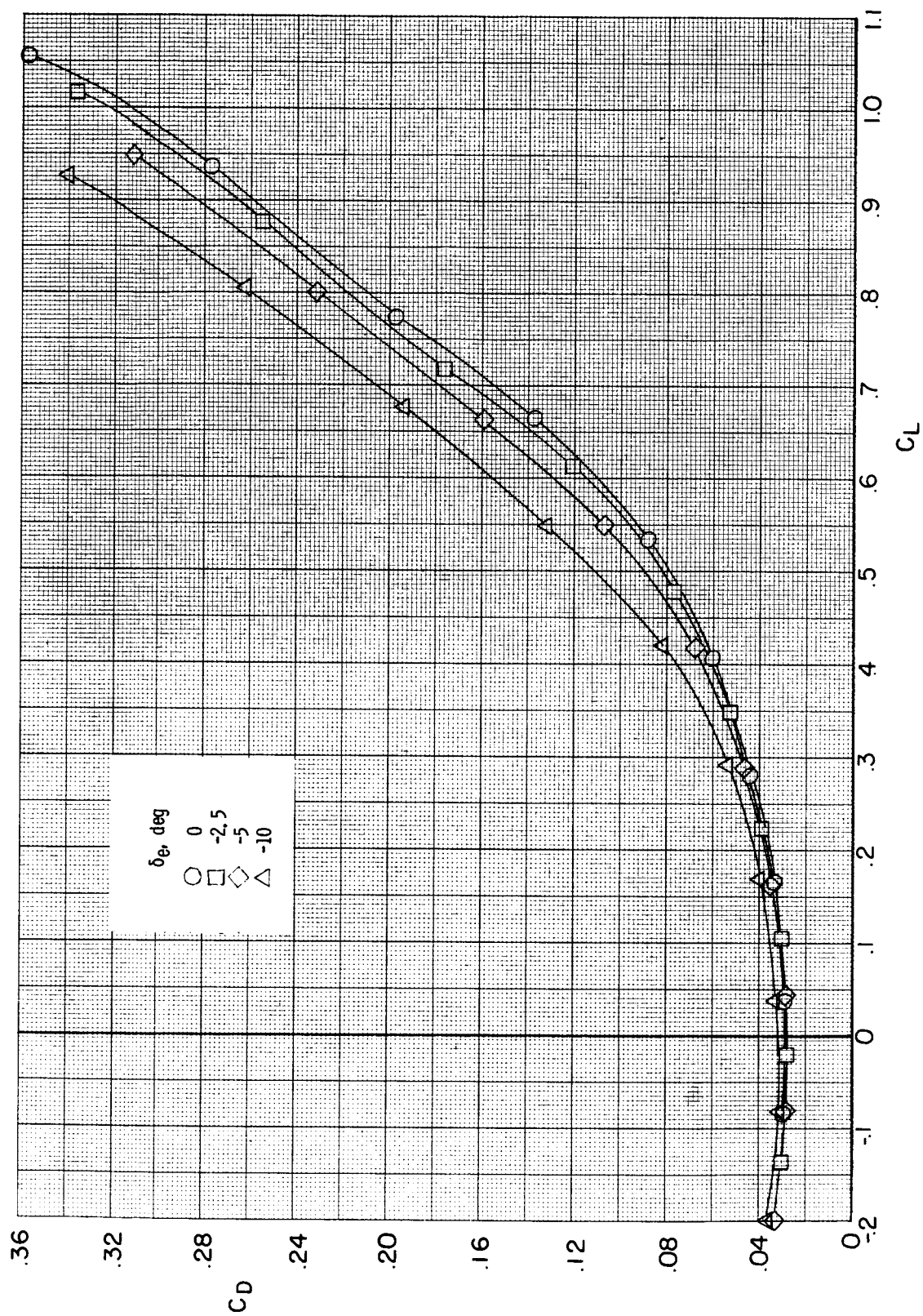


Figure 4.- Continued.



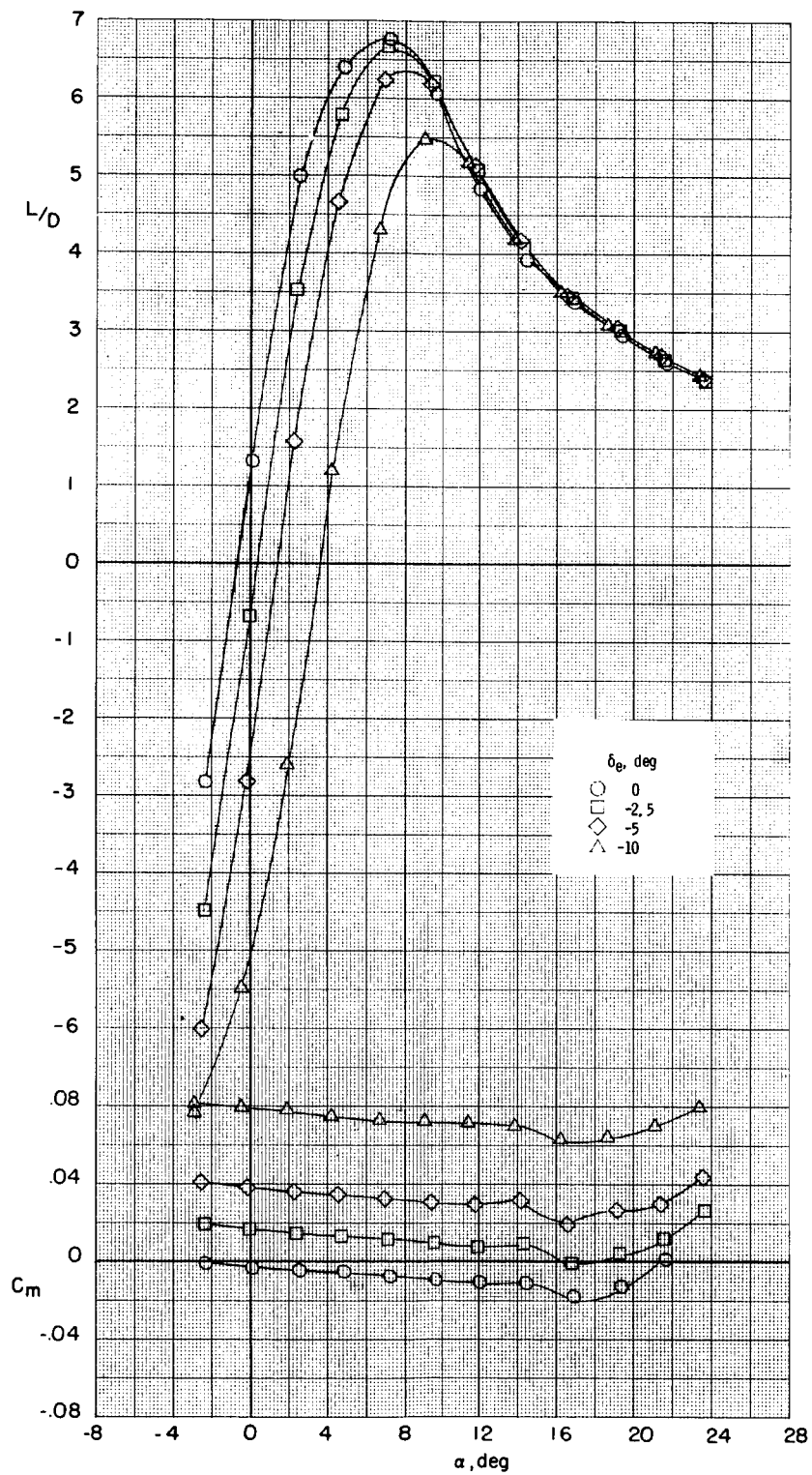


Figure 4.- Continued.

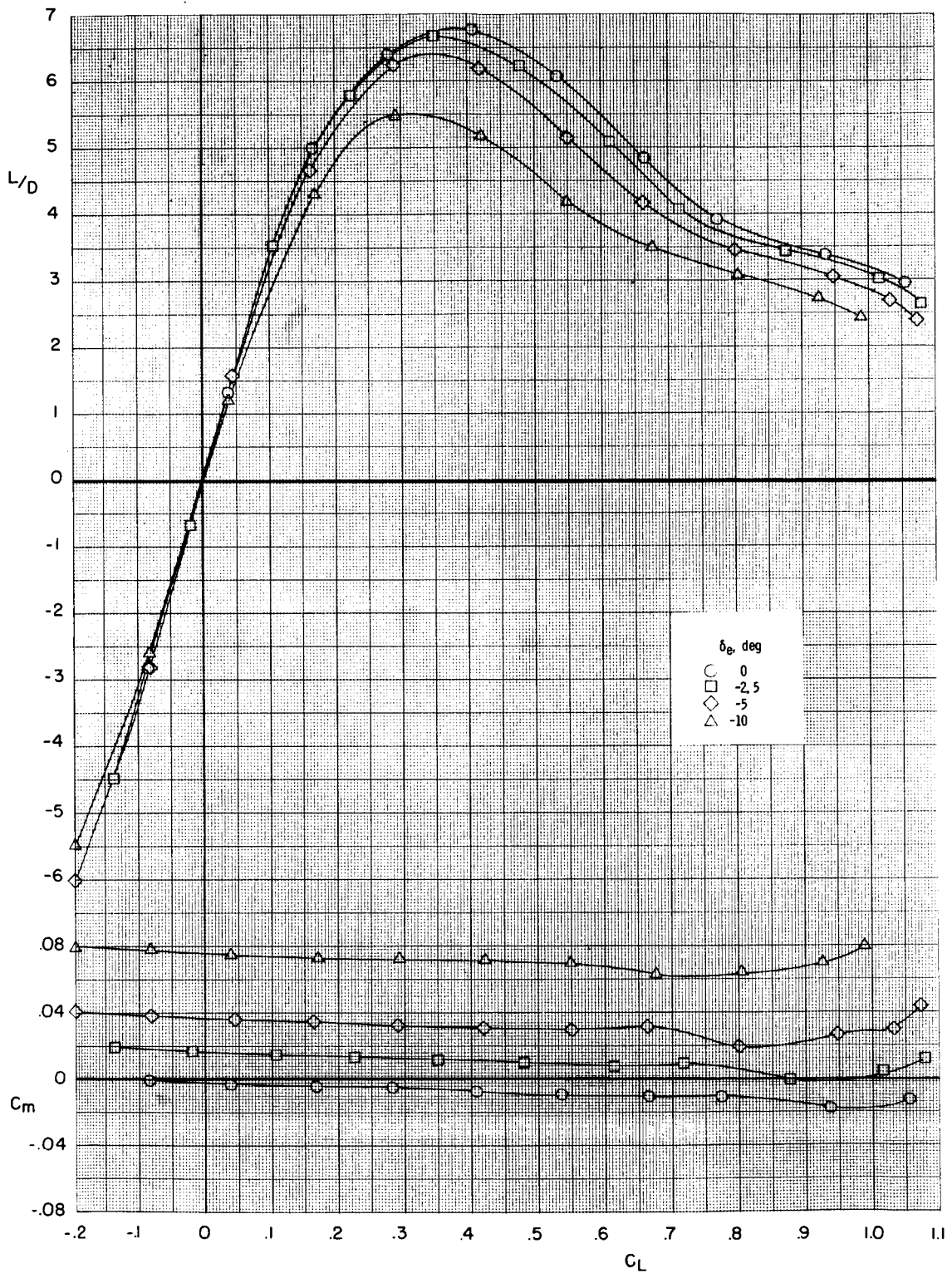


Figure 4.- Concluded.

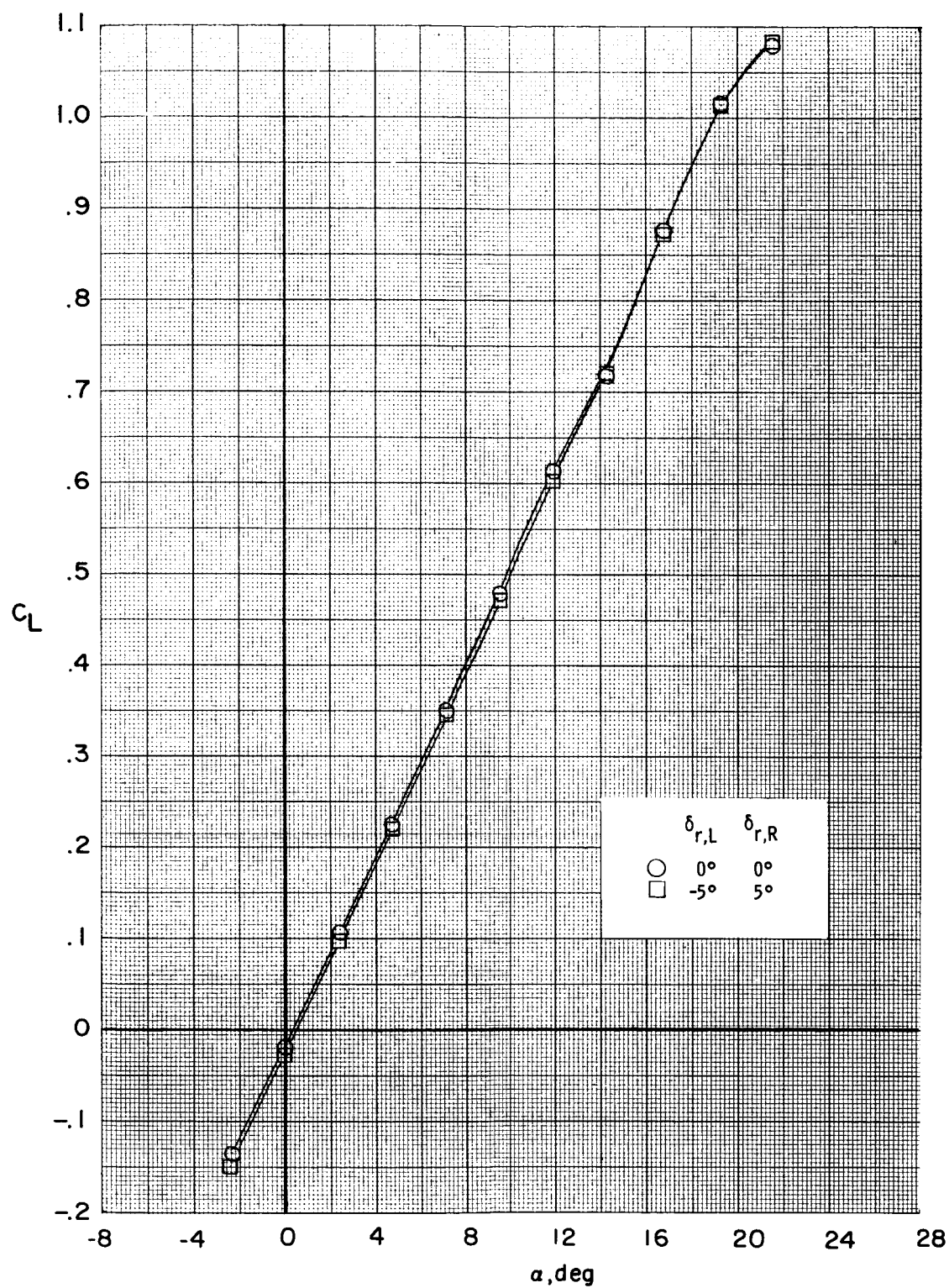


Figure 5.- Effects of rudders used as a pitch control on baseline model.  
 $R = 12.32 \times 10^6$ ;  $\beta = 0^\circ$ ;  $\delta_e = -2.5^\circ$ .

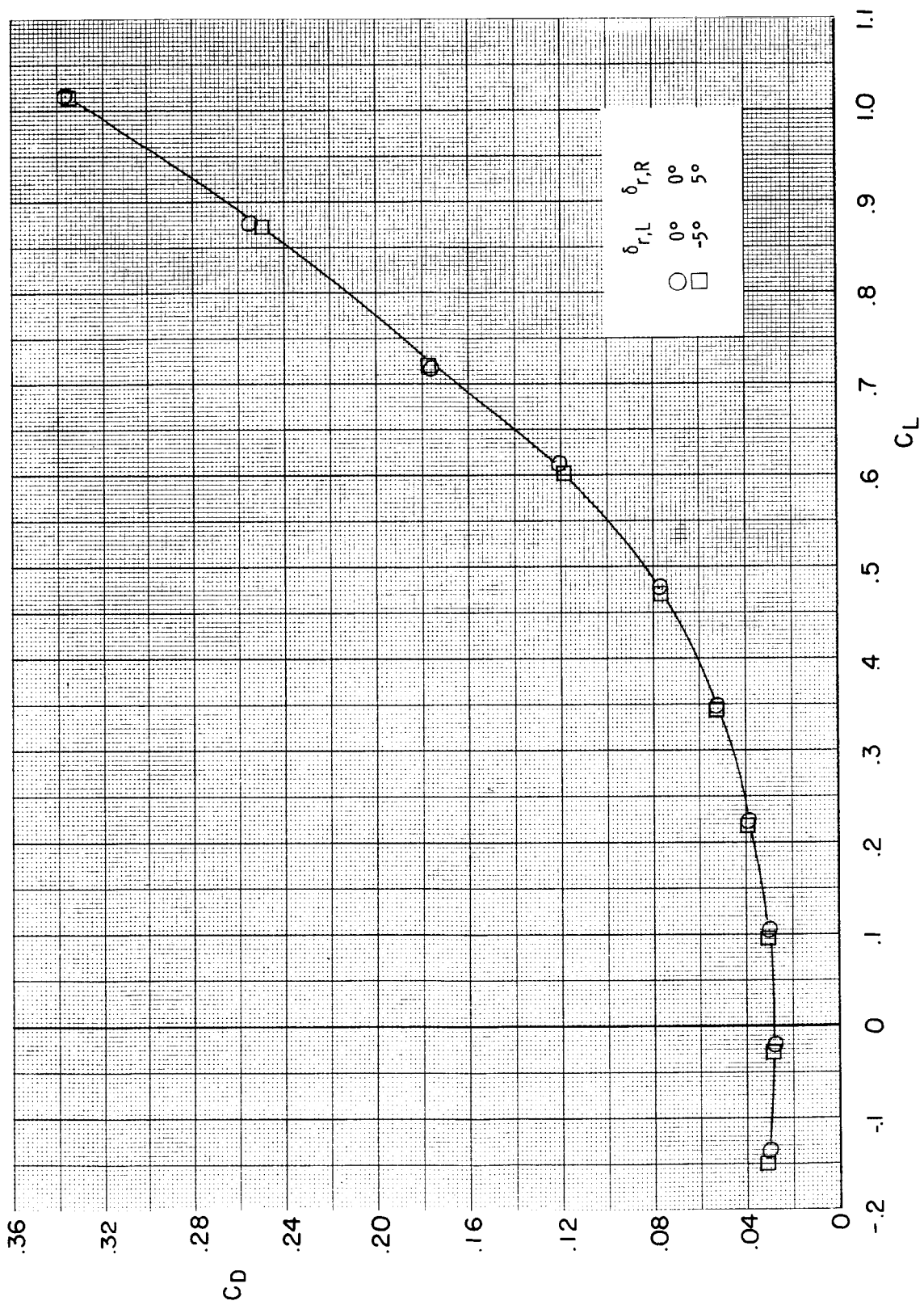


Figure 5.- Continued.

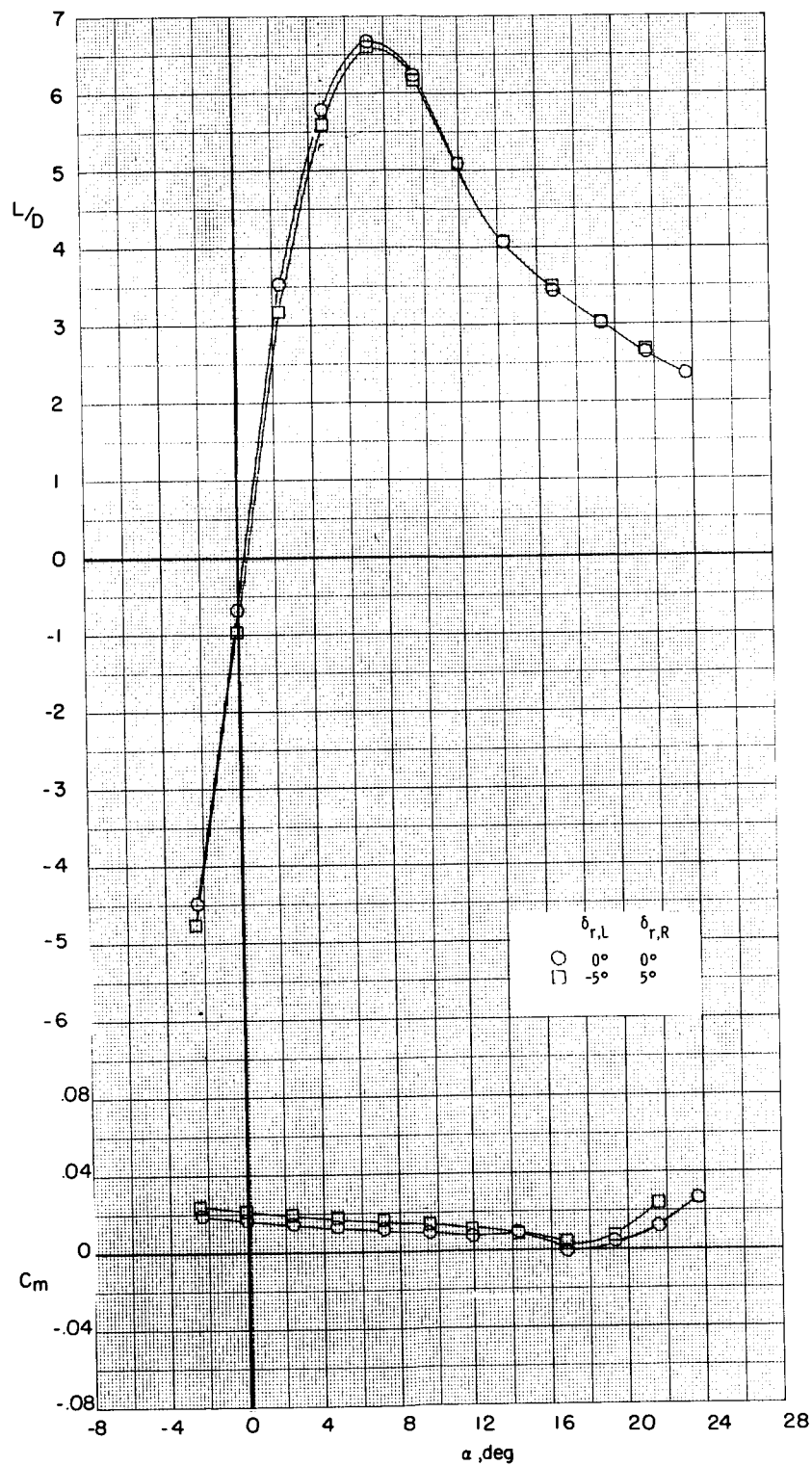


Figure 5.- Continued.

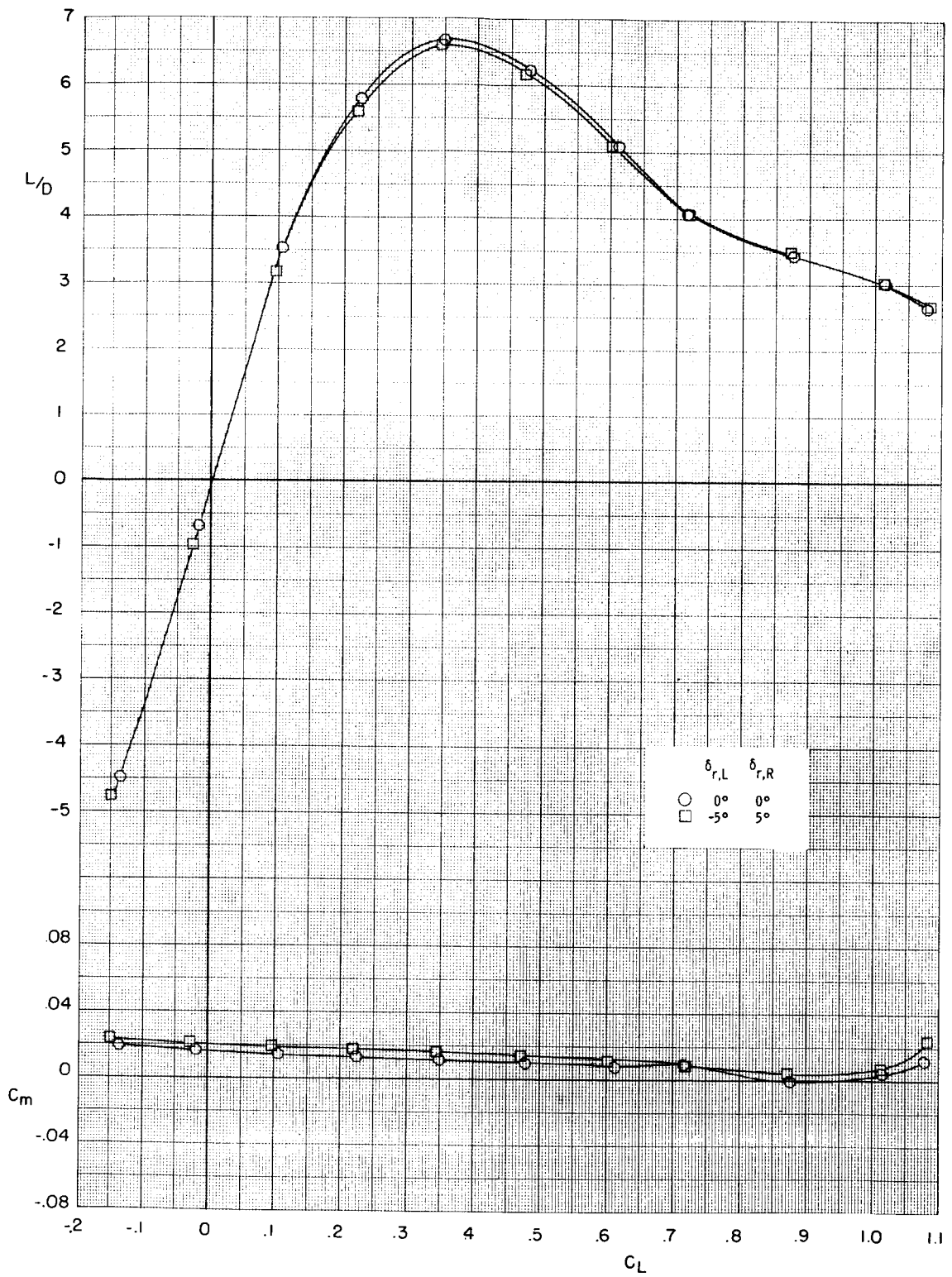


Figure 5.- Concluded.



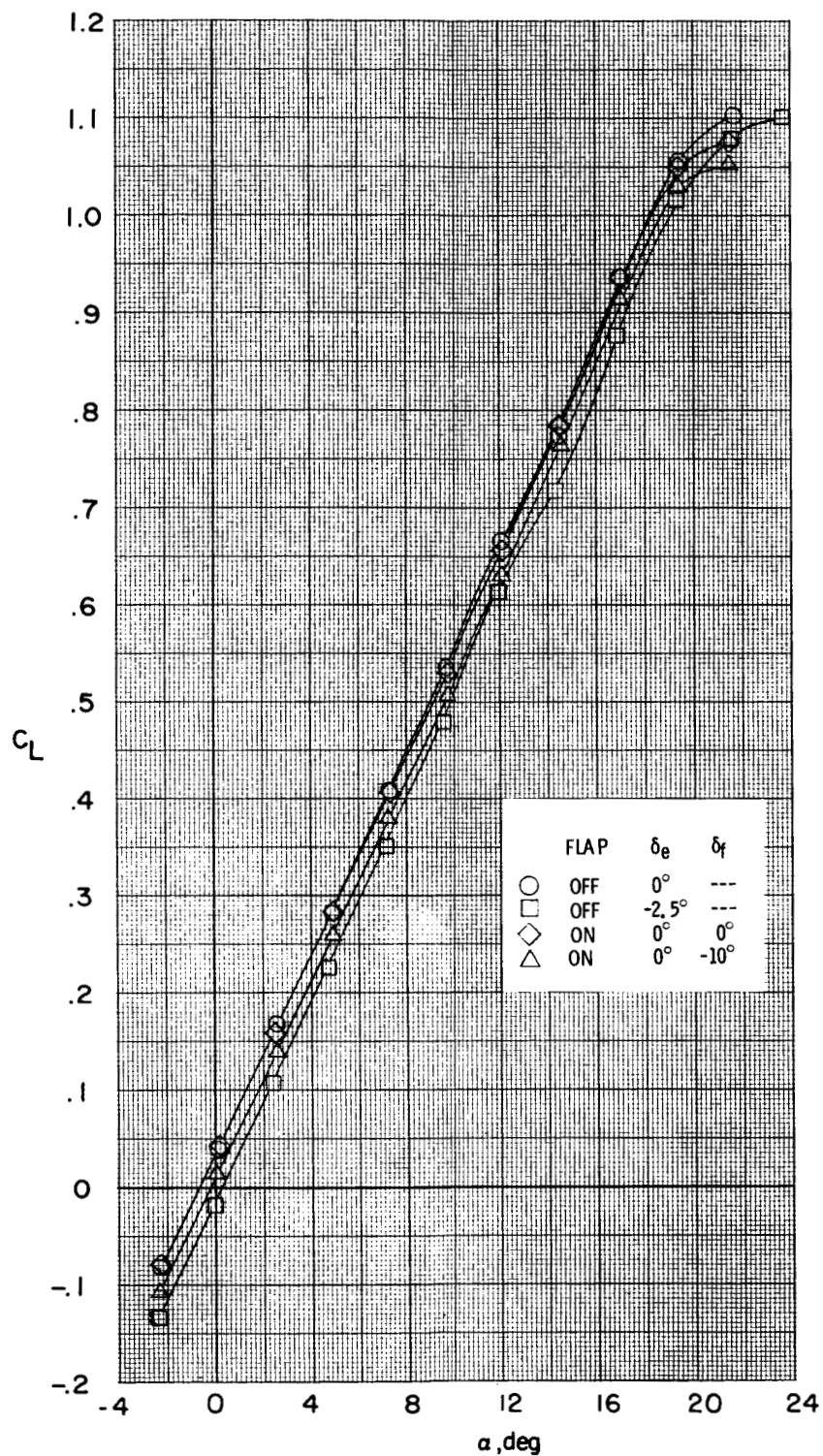


Figure 6.- Effects of addition and deflection of base flap on longitudinal aerodynamic characteristics of baseline model.  $R = 12.32 \times 10^6$ ;  $\beta = 0^\circ$ .

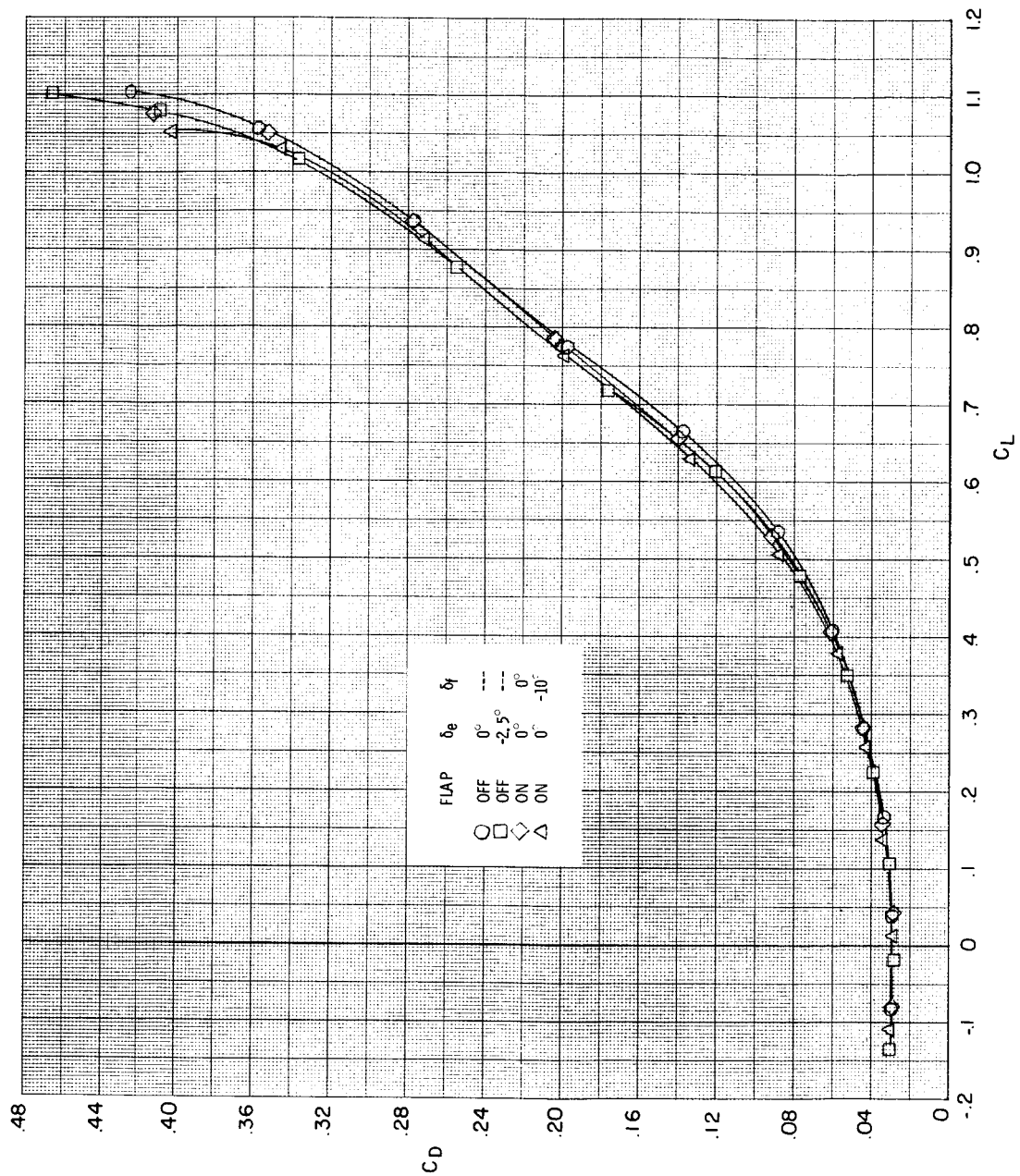


Figure 6.- Continued.



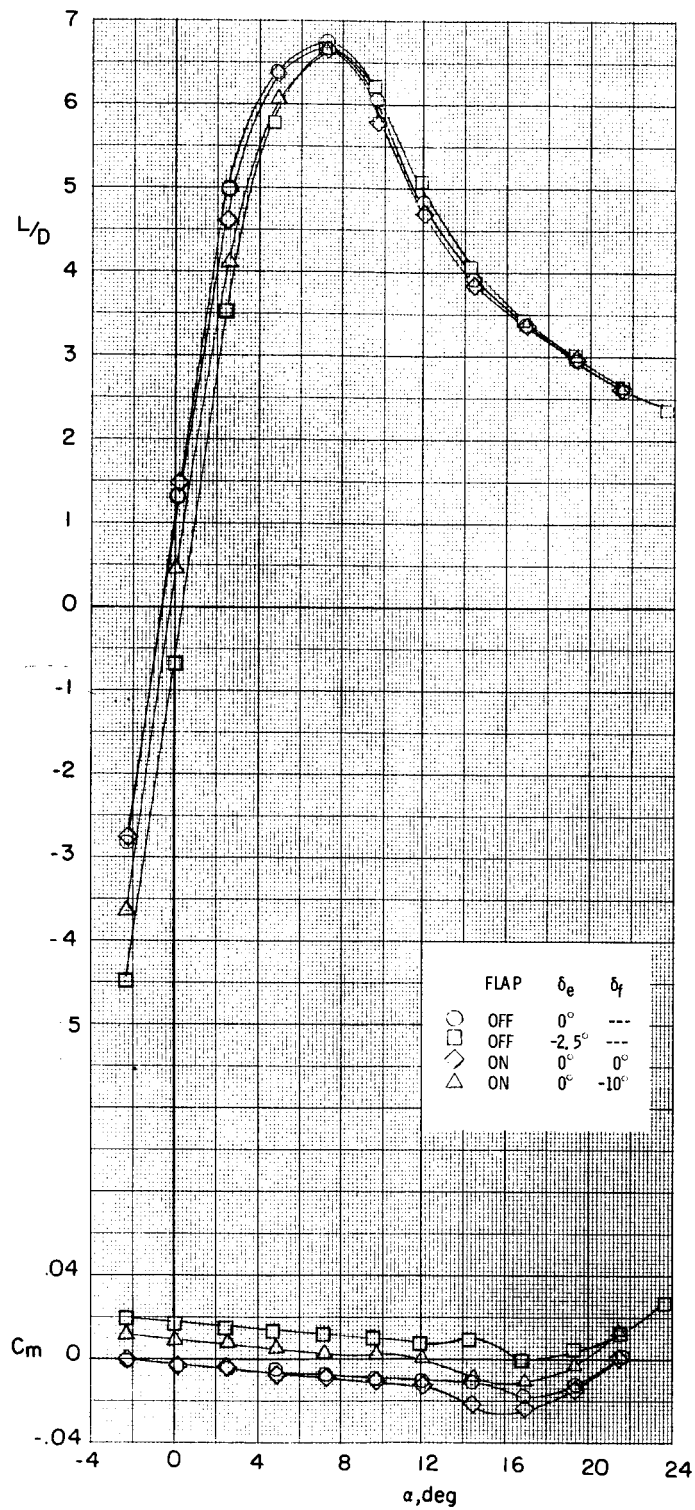


Figure 6.- Continued.

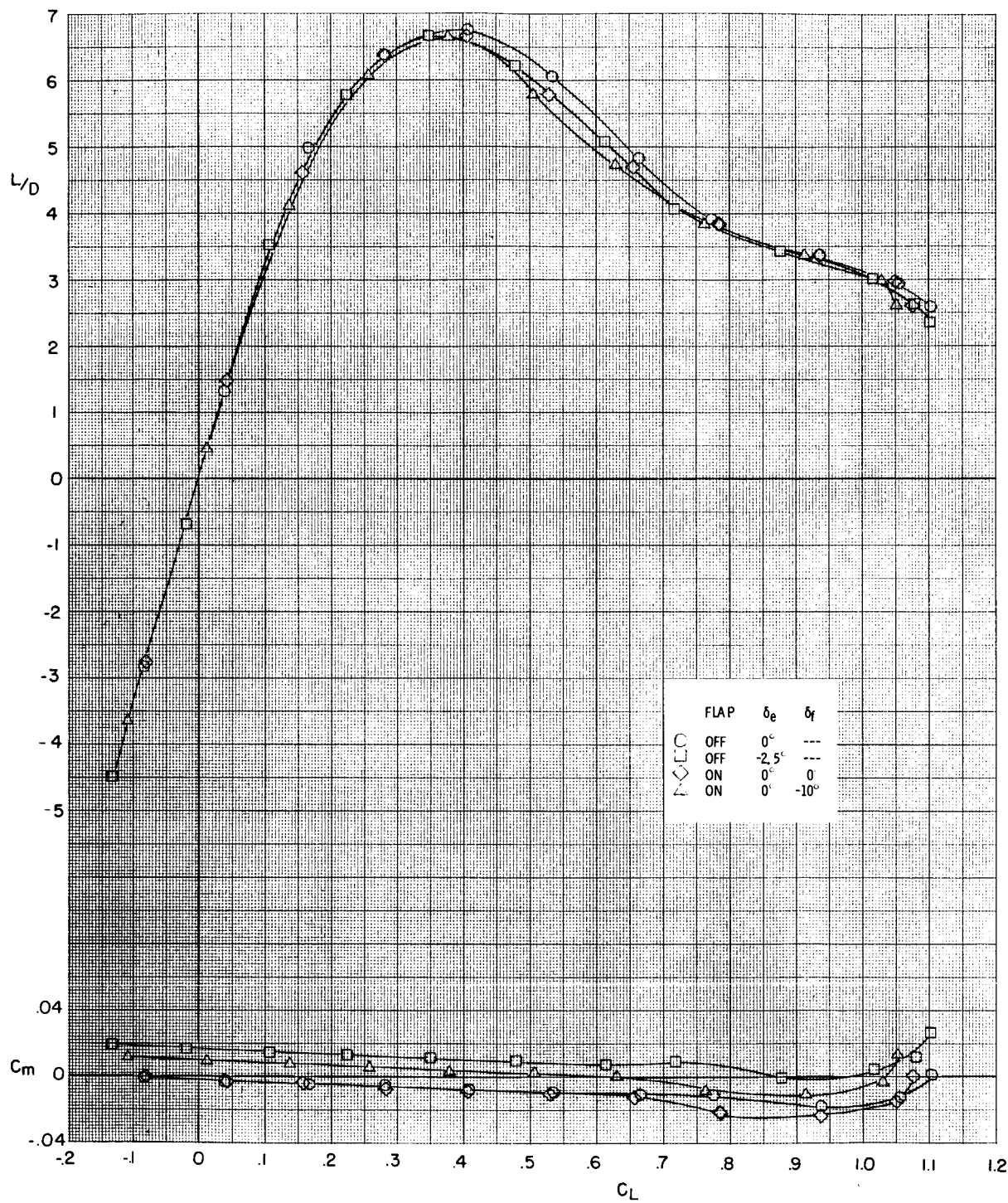


Figure 6.- Concluded.

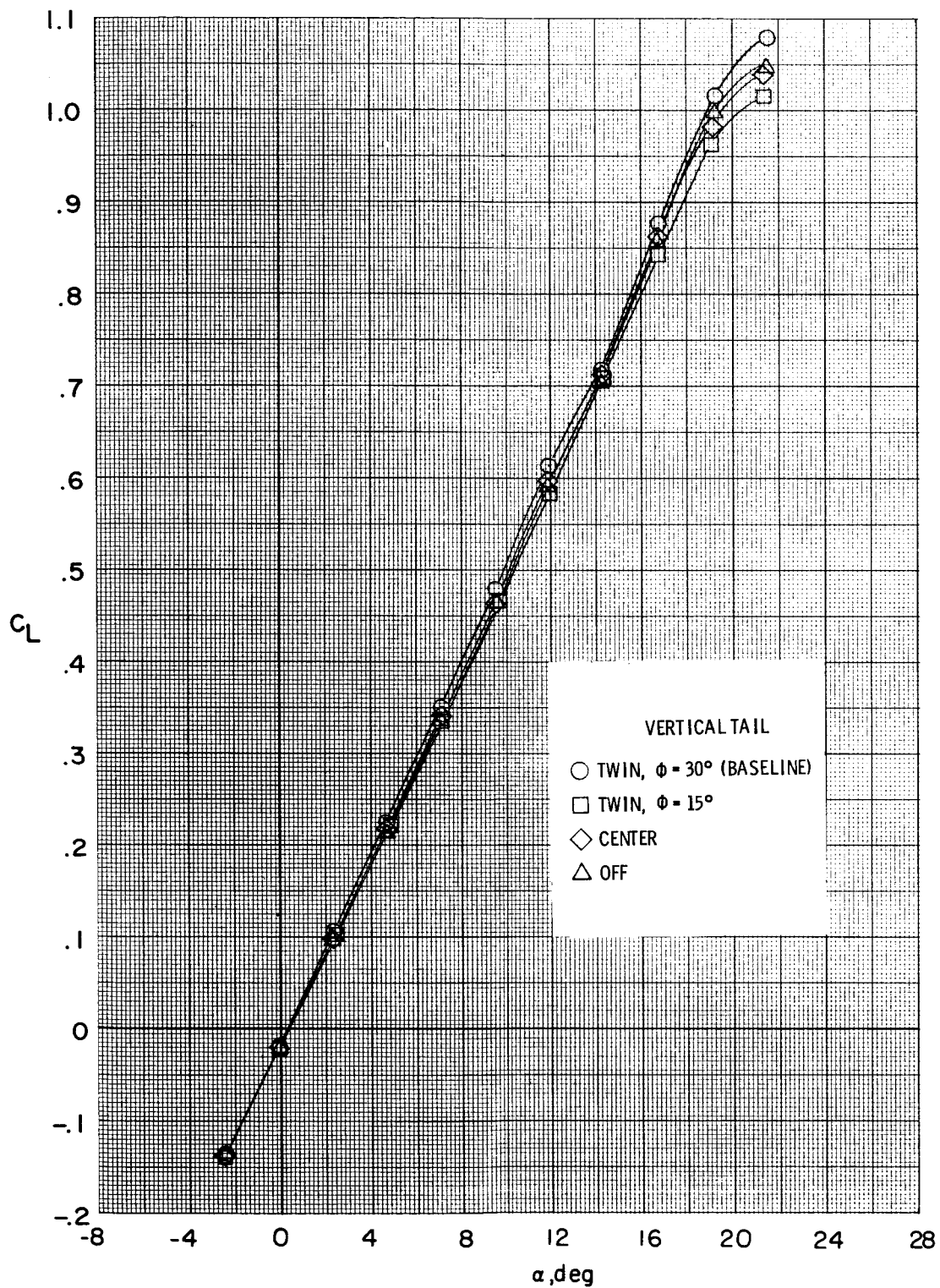


Figure 7.- Effects of vertical-tail configuration on longitudinal aerodynamic characteristics of baseline model.  $R = 12.32 \times 10^6$ ;  $\beta = 0^\circ$ ;  $\delta_e = -2.5^\circ$ .

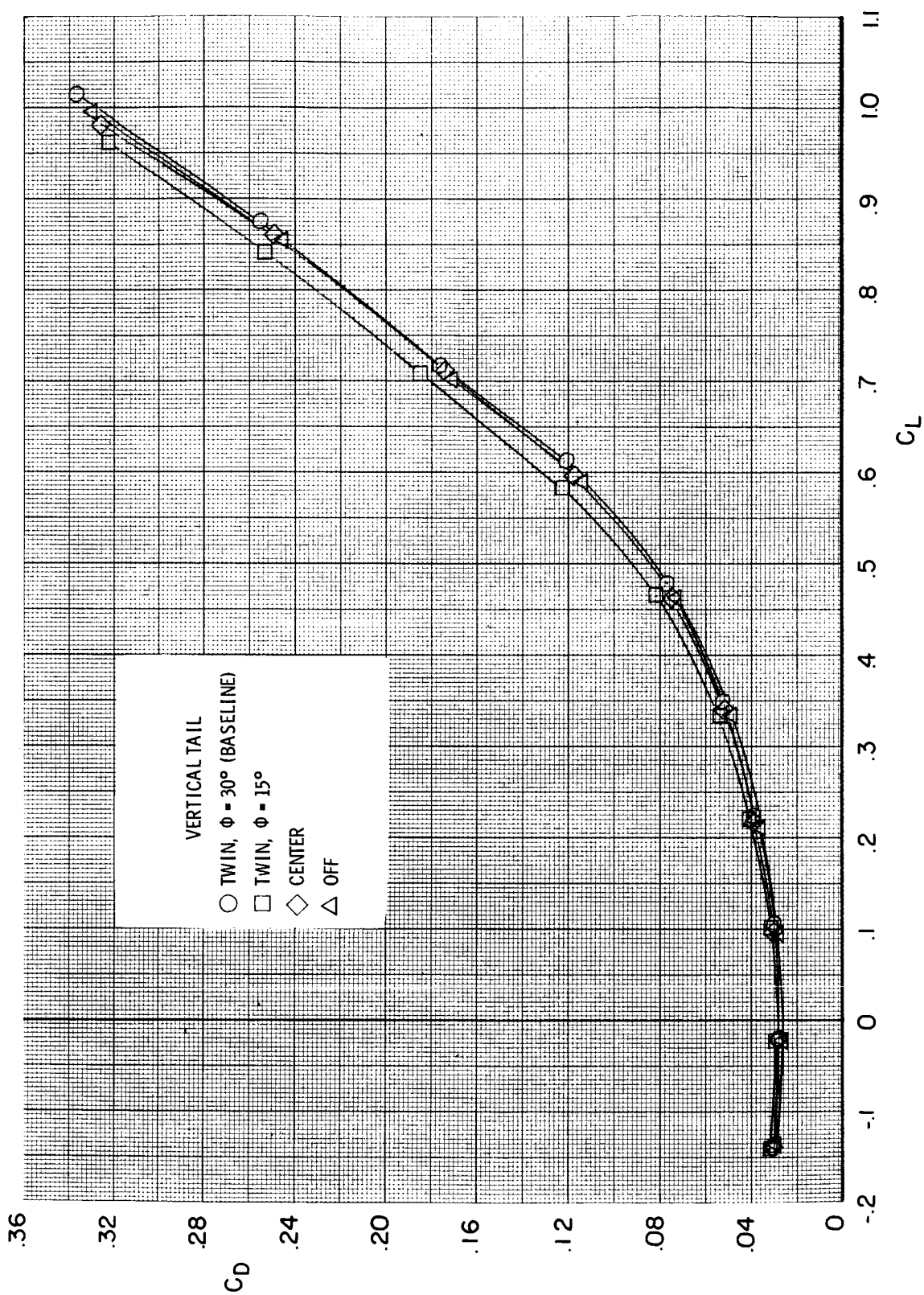


Figure 7.- Continued.

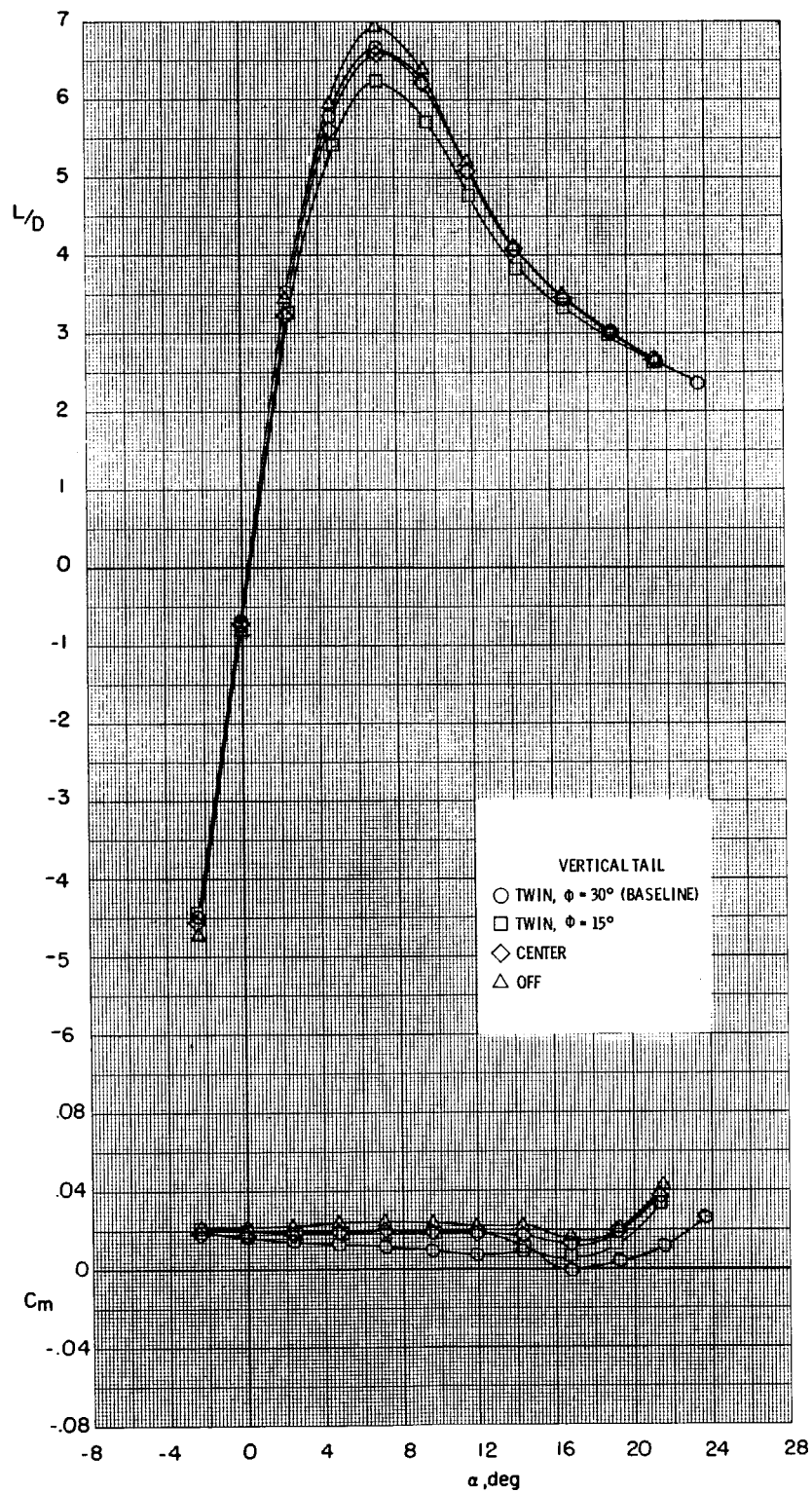


Figure 7.- Continued.



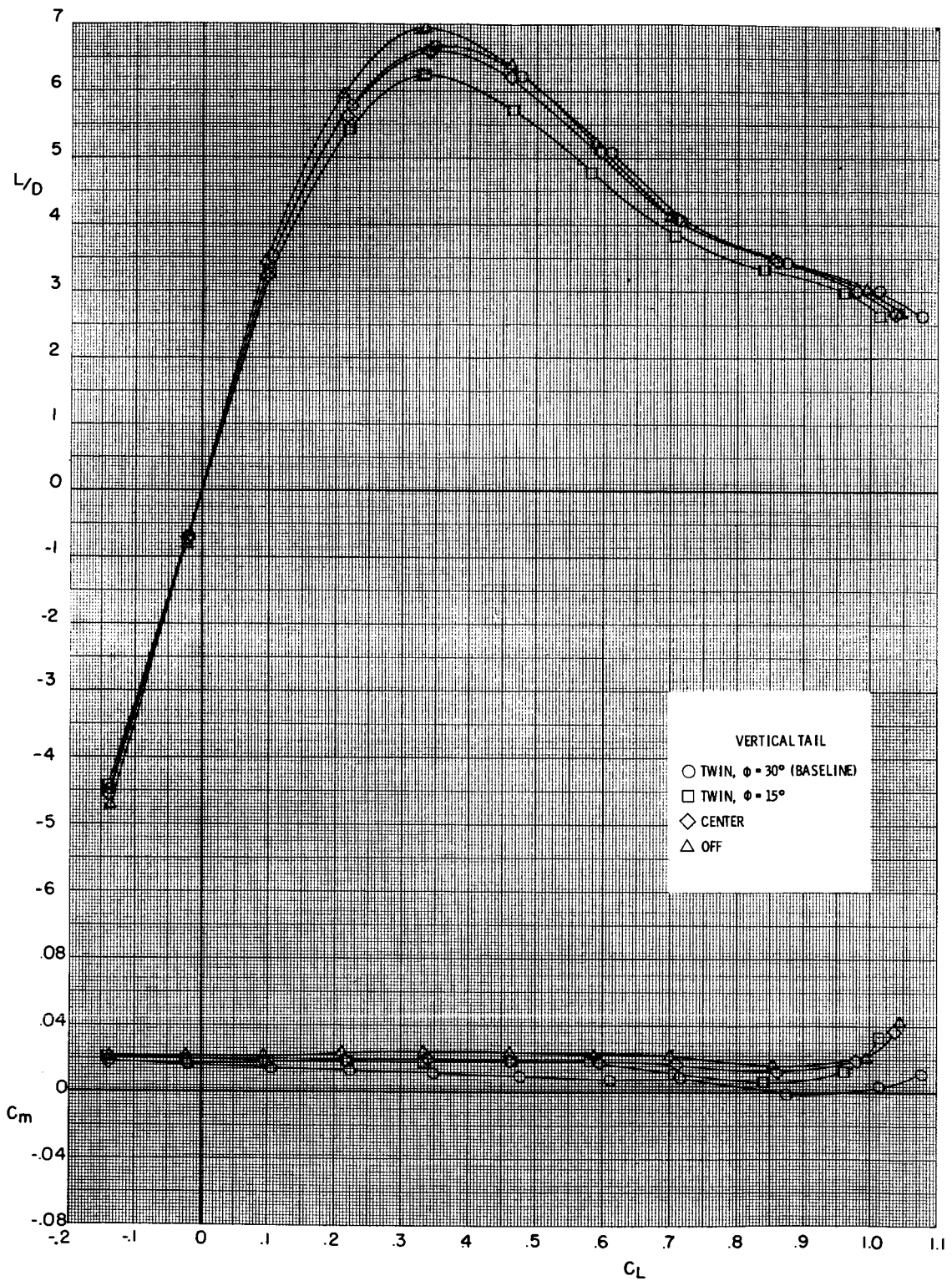


Figure 7.- Concluded.

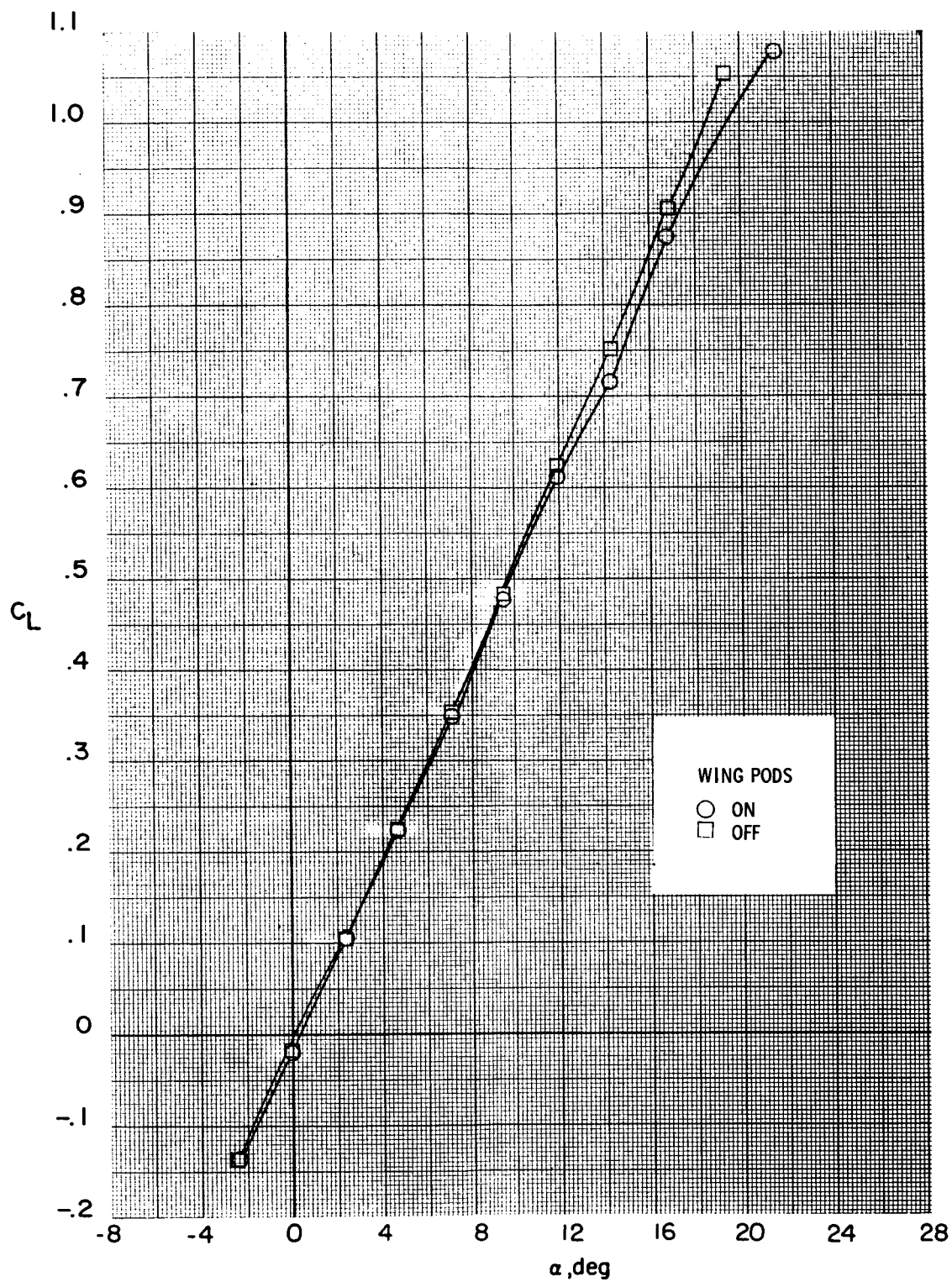


Figure 8.- Effects of wing pods on longitudinal aerodynamic characteristics of baseline model.  $R = 12.32 \times 10^6$ ;  $\beta = 0^\circ$ ;  $\delta_e = -2.5^\circ$ .

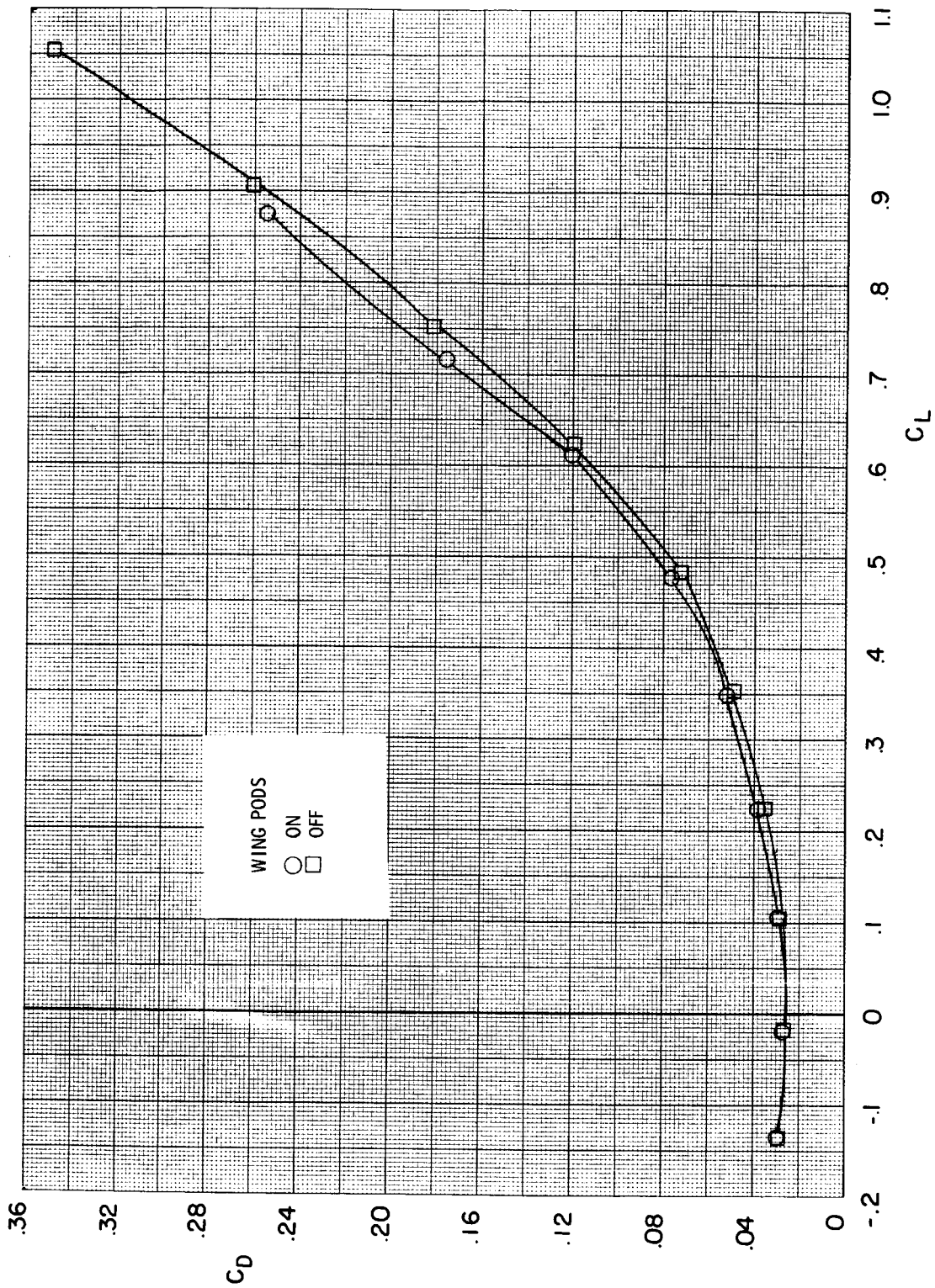


Figure 8.- Continued.



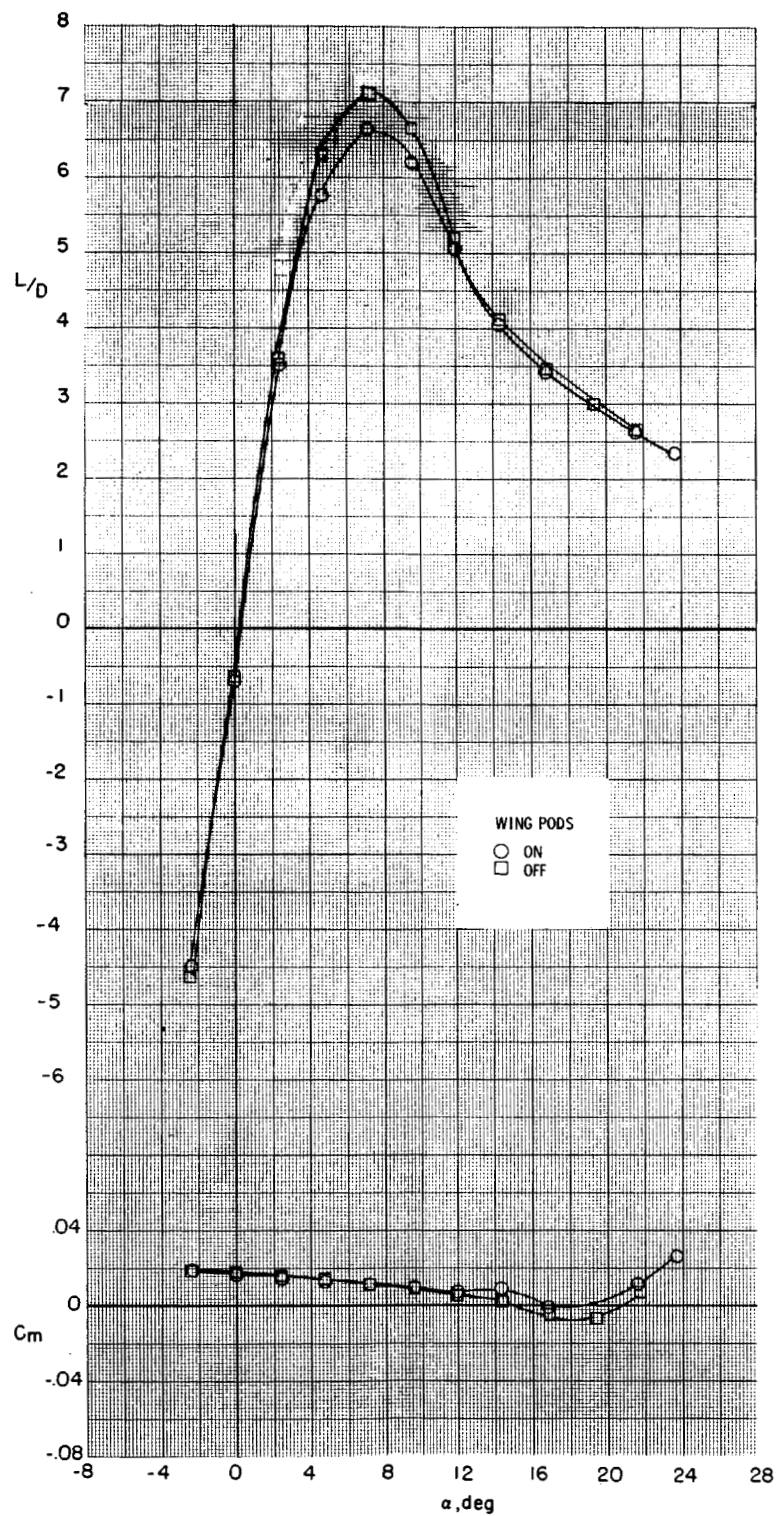


Figure 8.- Continued.

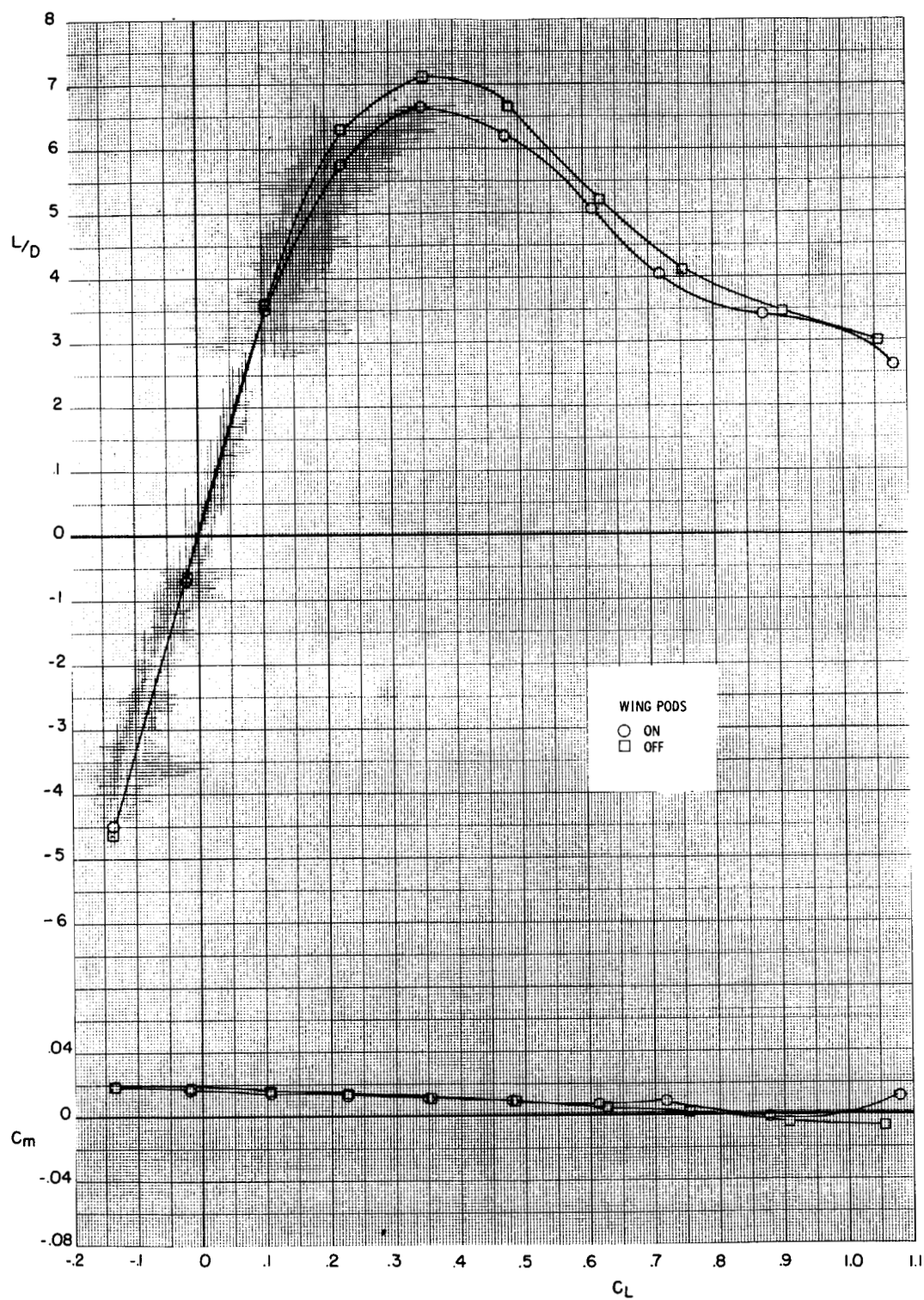


Figure 8.- Concluded.

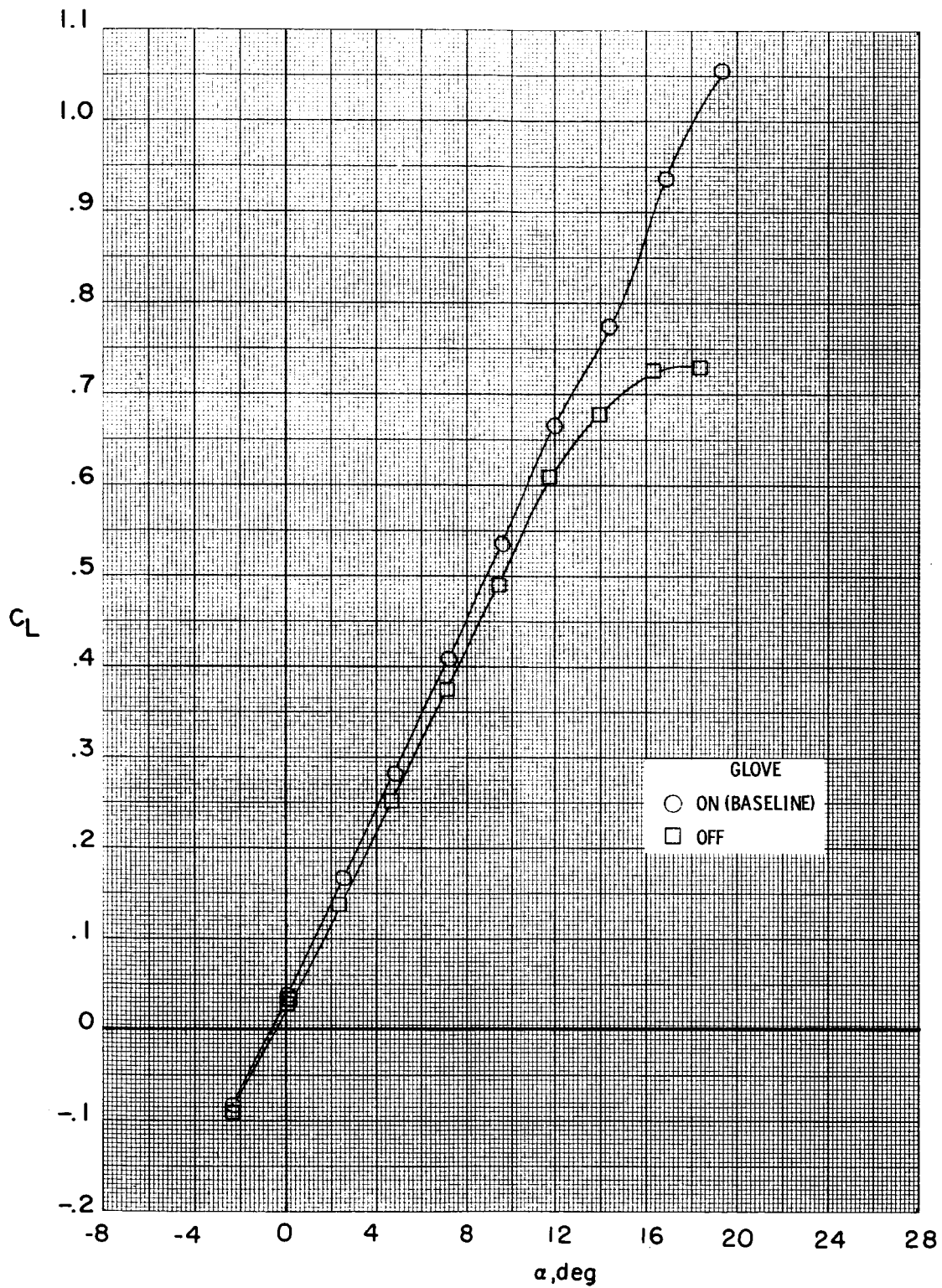


Figure 9.- Effects of wing planform on longitudinal aerodynamic characteristics of model.  
 $R = 12.32 \times 10^6$ ;  $\beta = 0^\circ$ ;  $\delta_e = 0^\circ$ .

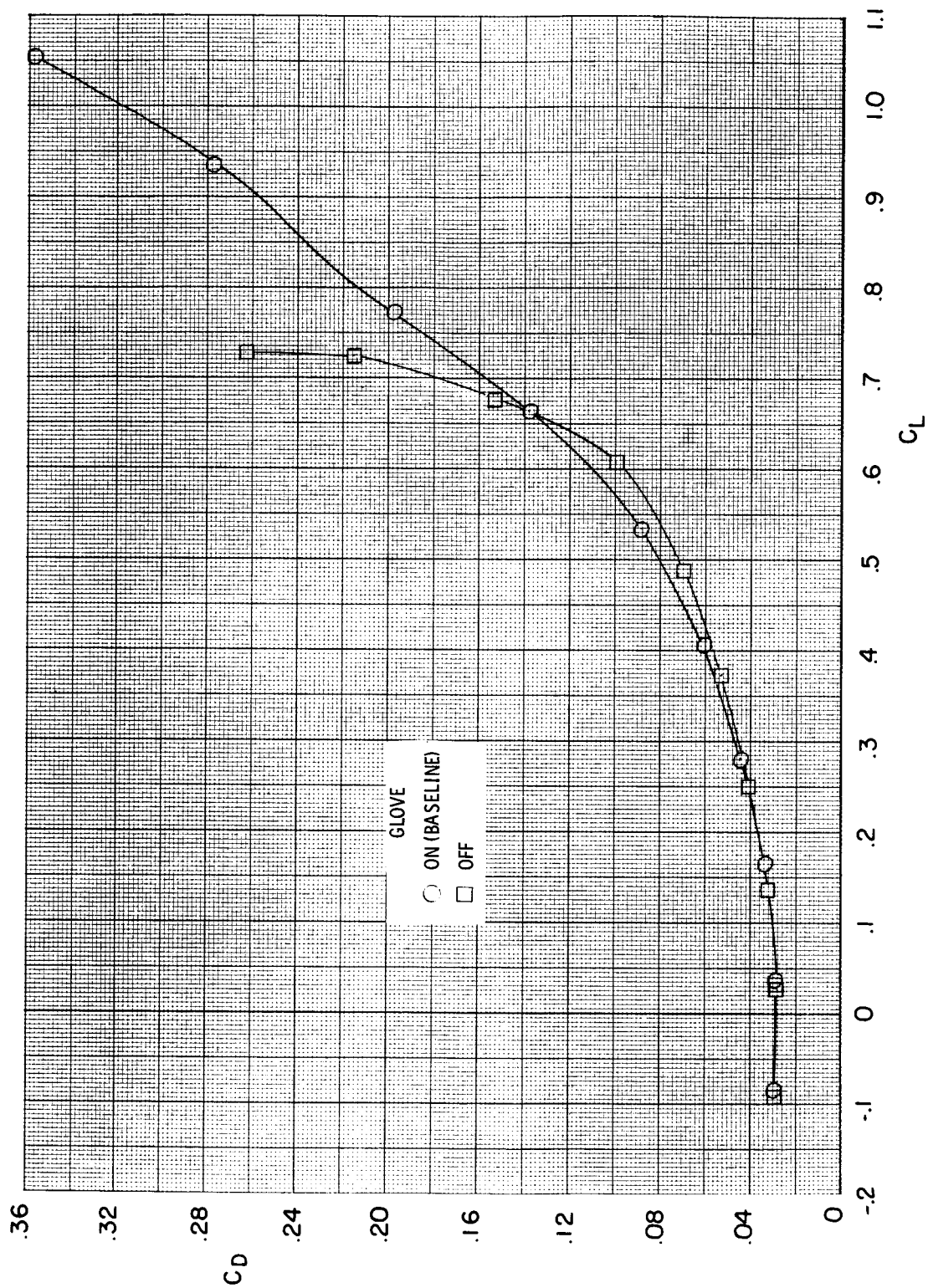


Figure 9.- Continued.

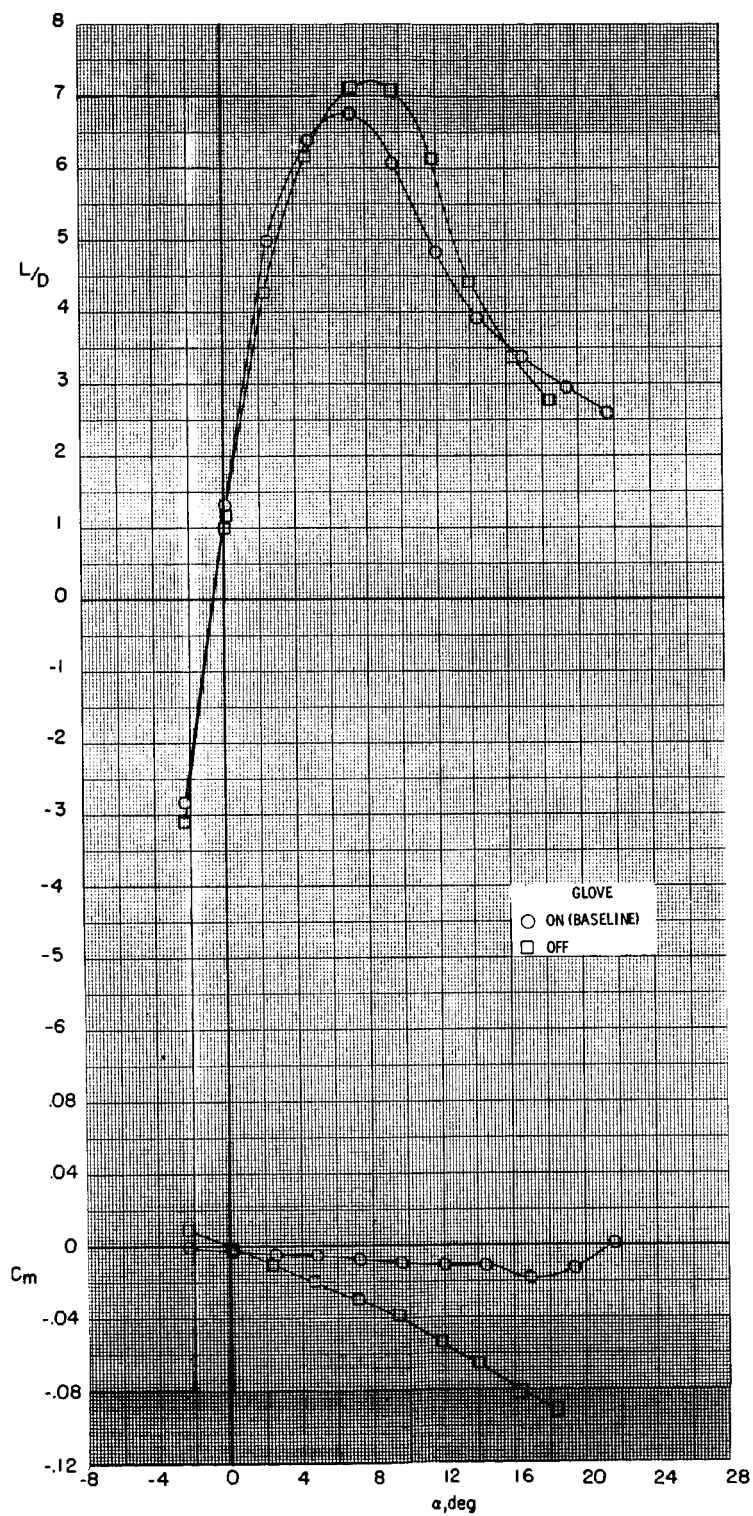


Figure 9.- Continued.



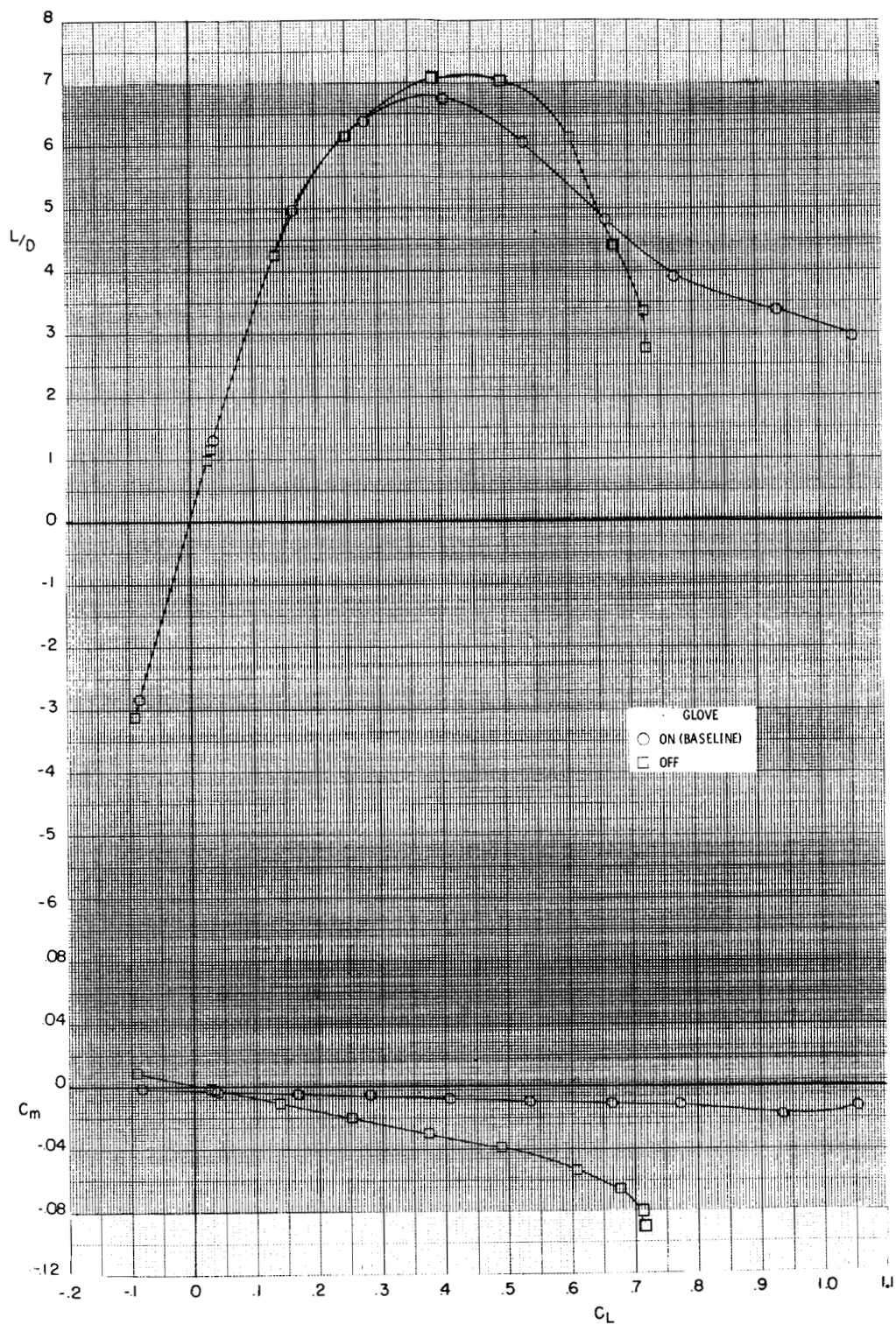


Figure 9.- Concluded.

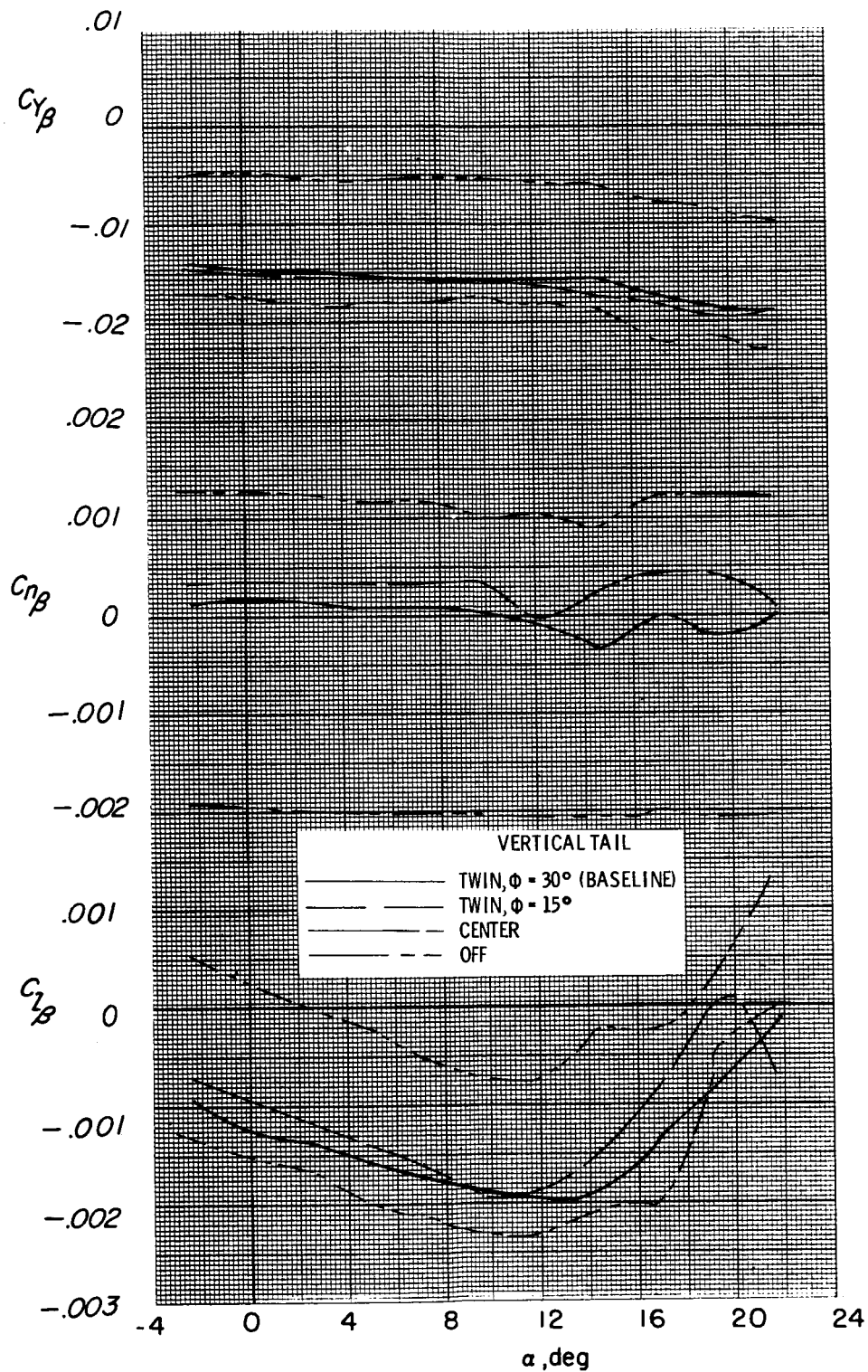


Figure 10.- Effects of vertical-tail configuration on lateral-directional aerodynamic characteristics of model with wing glove on.  $R = 12.32 \times 10^6$ ;  $\delta_e = -2.5^\circ$ .

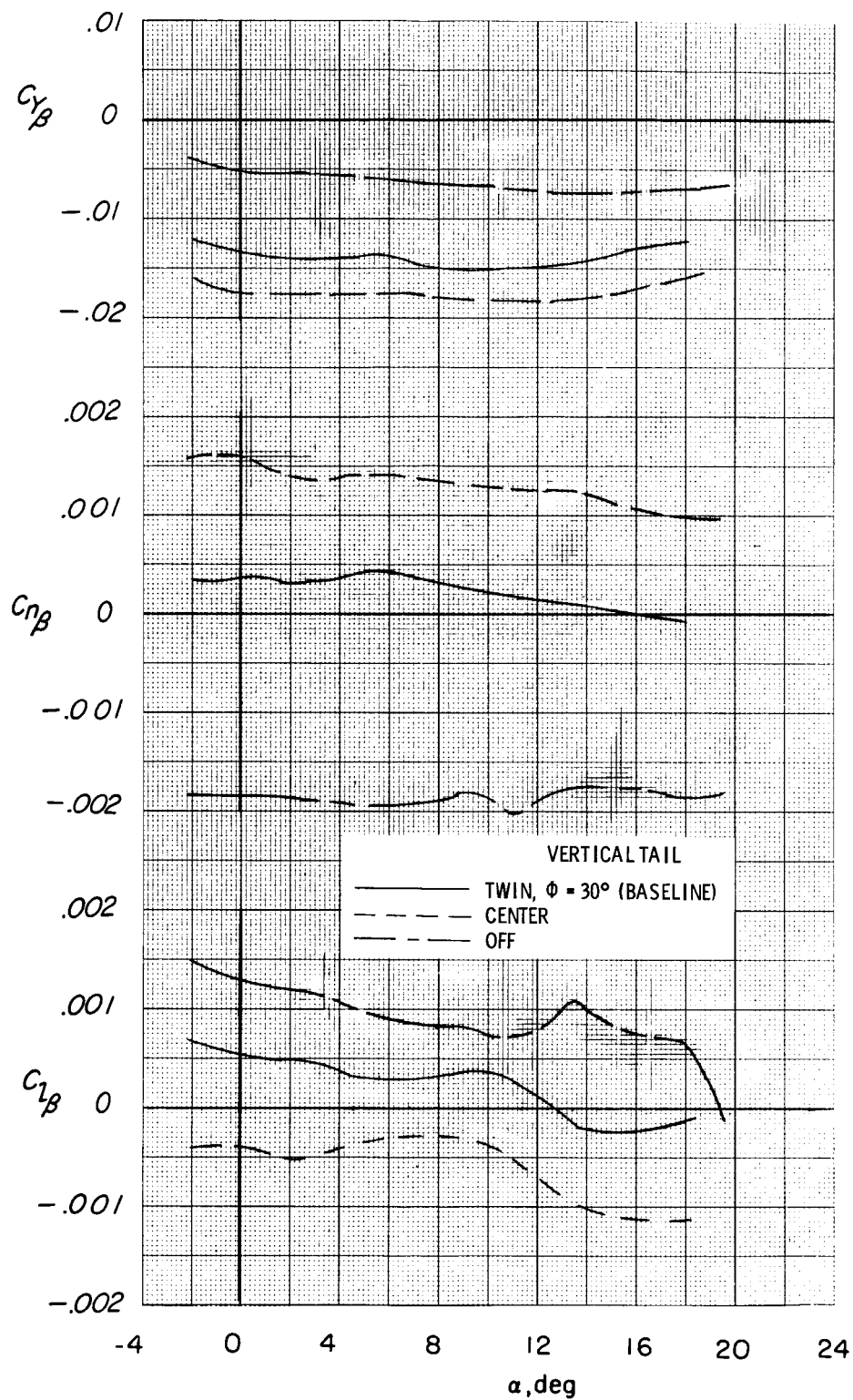


Figure 11.- Effects of vertical-tail configuration on lateral-directional stability characteristics of model with glove off.  $R = 12.32 \times 10^6$ ;  $\delta_e = -2.5^\circ$ .